Laramide minor faulting in the Colorado Front Range

Eric A. Erslev, Steven M. Holdaway[1], Stephanie A. O'Meara[2],
Branislav Jurista[3], and Bjorn Selvig[4]

Department of Earth Resources, Colorado State University, Fort Collins, CO 80523
[1]Now at Chevron USA Production Company, P.O. Box 36366, Houston, TX 77236
[2]Now at Colorado State University/National Park Service, 1201 Oak Ridge Drive, Suite 200, Fort Collins, CO 80525
[3]Now at Westshore Consulting, 2534 Black Creek Road, Muskegon, MI 49444
[4]Now at RETEC, 23 Old Town Square, Suite 250, Fort Collins, CO 80524

Abstract

The nature of Laramide basement-involved deformation in the Rocky Mountains remains highly controversial, sparking a continuing debate between advocates of vertical, thrust and strike-slip tectonic models. The Front Range of Colorado provides an important geographic link between the northwest-trending arches of Wyoming, which are commonly attributed to thrust deformation, and the north-trending arches of the southern Rockies of New Mexico, which are commonly attributed to partitioned right-lateral transpression.

Fault separations and kinematics provide effective tests of Laramide structural models for the Front Range arch. In the center of the arch, exposures of Precambrian crystalline rocks show no evidence of consistent strike-slip separations on north-striking faults, indicating that major right-lateral displacements, if present, must be located on the margins of the arch. Fault kinematics were studied by measuring nearly 5,000 slickensided faults in Mesozoic strata flanking the Front Range arch. The overwhelming dominance of thrust and strike-slip minor faults with low-angle slickenline plunges falsifies vertical tectonic hypotheses invoking dip-slip on high-angle faults. Average slickenline and ideal σ_1 axis trends for the minor faults range from N53°E to N80°E, with some variability due to localized folding and faulting. The high intersection angles of average slickenline and compression orientations with major fault strikes suggest a predominance of thrust motion on the bounding faults of the Front Range arch. The lack of north-striking, strike-slip minor faults of clear Laramide age indicates that slip partitioning was not a major contributor to regional Laramide deformation in the Colorado Front Range. The slight obliquity between the arch axis and average slickenline and compression orientations is consistent, however, with a minor component of right-lateral slip on the thrust faults that bound the Front Range of Colorado.

Introduction

The Colorado Front Range (Fig. 1) is an important yet controversial part of the Rocky Mountain foreland. Its location adjacent to the Denver geological community, with its strong academic, industry, and U.S. Geological Survey components, has made the Front Range an important influence in defining our understanding of basement-involved foreland arches. Field observations from the eastern Front Range played a key role in the development of the vertical uplift school of Laramide deformation (Prucha et al. 1965; Matthews and Work 1978) and subsequent strike-slip hypotheses (Chapin and Cather 1981; Chapin 1983), which used Front Range geologic relationships to support northward translation of the Colorado Plateau during the Laramide orogeny.

This paper will synthesize 10 years of minor fault studies at Colorado State University that were aimed at testing hypotheses for the Laramide formation of the Front Range of Colorado. The premise of this paper is that many structural models for the Laramide development of the Front Range predict significantly different stresses and strains, which can be deduced from the characteristics of minor faults. Details of this research are partially contained in five M.S. theses (Selvig 1994; Jurista 1996; Fryer 1997; Holdaway 1998) as well as several society field trip articles (Erslev and Gregson 1996; Erslev and Selvig 1997; Erslev and Holdaway 1999; Erslev et al. 1999). This work is part of the larger Continental Dynamics—Rocky Mountain Project (CD-ROM) studying the Rocky Mountain lithosphere from its Precambrian assembly to the present. The CD-ROM project is combining the fault data presented here with diverse geological and geophysical studies to help delineate the geologic evolution of the Southern Rocky Mountains.

Geologic setting and structural models

The Rocky Mountain province of the United States is a classic basement-involved foreland orogen. Deformation during the Late Cretaceous to Eocene Laramide orogeny created an anastomosing system of basement-cored arches that bound the northern and eastern margins of the Colorado Plateau and define the elliptical sedimentary basins of the Rocky Mountains. The tectonic mechanism for Laramide deformation remains controversial with proposed mechanisms ranging from subcrustal shear during low-angle subduction (Bird 1988, 1998; Hamilton 1988) to detachment of the upper crust during plate coupling to the west (Lowell 1983; Oldow et al. 1989; Erslev 1993). The Southern Rocky Mountains, here defined as the Rocky Mountains south of Wyoming, have been further complicated by multiple stages of Tertiary faulting, igneous activity and sedimentation currently manifested by the Rio Grande rift.

The multitude of Laramide structural geometries in the Rocky Mountains has resulted in a mirroring multitude of kinematic hypotheses. In the 1970s and 1980s hypotheses were polarized into the antagonistic horizontal compression and vertical tectonics schools. The vertical tectonics school was dominant in the 1970s, represented by upthrust (Prucha et al. 1965) and block uplift models (Stearns 1971, 1978; Matthews and Work 1978). In the 1980s incontrovertible documentation of Precambrian basement thrust over Phanerozoic sediments (e.g., Smithson et al. 1979; Gries 1983; Lowell 1983; Stone 1985) swung opinion back toward models invoking horizontal shortening and compression. Seismic profiles (Smithson et al. 1979; Gries and Dyer 1985), subthrust petroleum drilling at Laramide basin margins (Gries 1983), and balancing constraints (Stone 1984; Brown 1984; Erslev 1986; Spang and Evans 1988) have demonstrat-

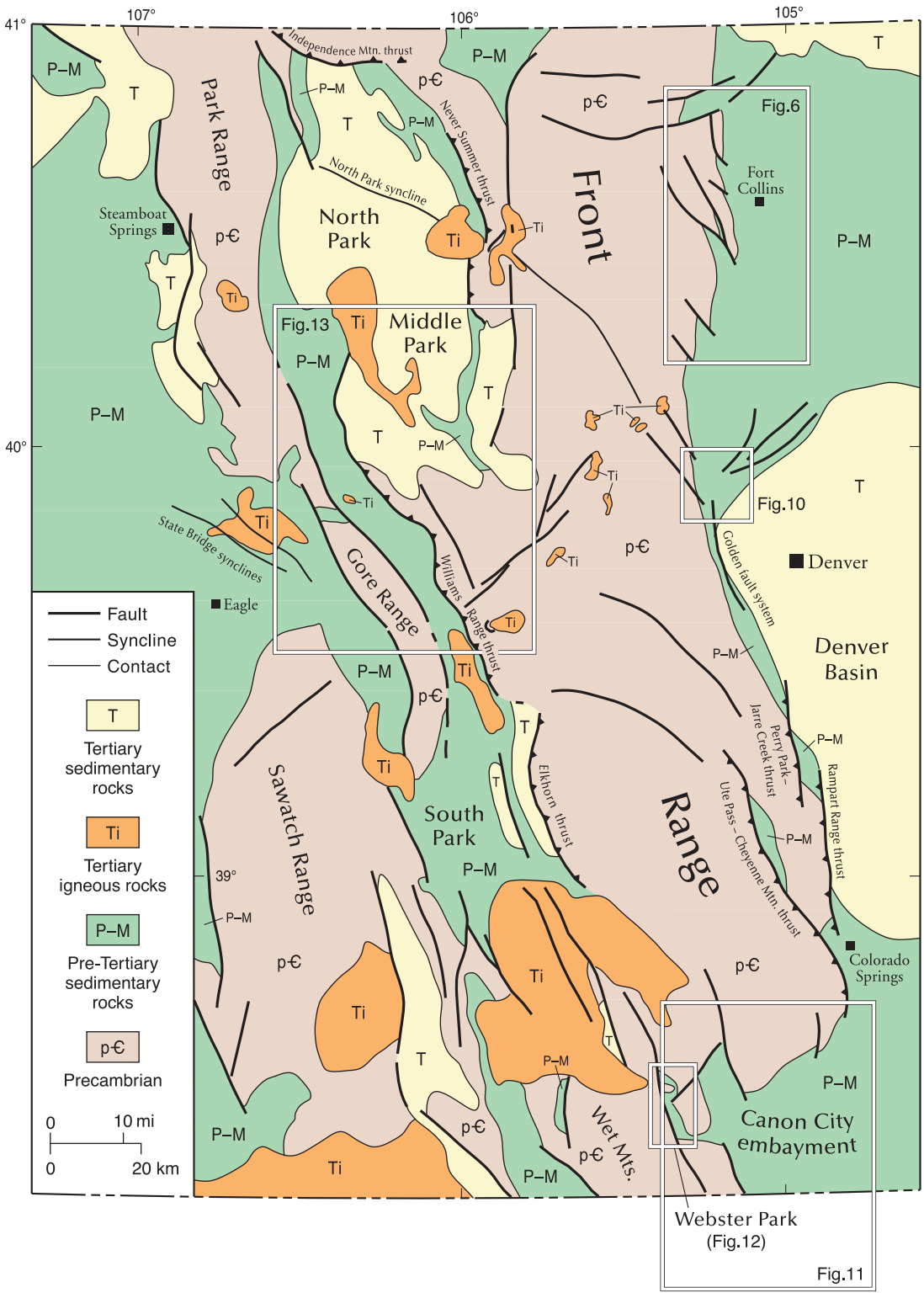

FIGURE 1—Geologic map of the Colorado Front Range (simplified from Tweto 1979) with boxes indicating areas of more detailed maps contained within subsequent figures.

ed that the Laramide was dominated by lateral shortening due to horizontal compression.

The diversity of Laramide structural trends, with faults, folds, and arches trending in nearly every direction, has been attributed to multiple stages of differently oriented compression (Chapin and Cather 1981; Gries 1983; Bergh and Snoke 1992), reactivation of pre-existing weaknesses in the basement (Hansen 1986; Stone 1986; Blackstone 1990; Chase et al. 1993), transpressive motions (Cather 1999a,b), indentation by the Colorado Plateau (Hamilton 1988), and detachment of the crust (Lowell 1983; Brown 1988; Kulik and Schmidt 1988; Oldow et al. 1990; Erslev 1993). Many of

these hypotheses are valid for individual areas within the foreland but their relative regional importance is not always clear.

Laramide structures of the Front Range basement arch (Fig. 1) are very diverse. Along the eastern flank of the range, the north-northwest-striking, west-dipping Golden thrust fault system (Berg 1962) west and south of Denver transitions to an array of northwest-striking, east-dipping reverse faults to the north (Erslev 1993). Farther south, the Golden fault system merges into the Perry Park–Jarre Creek and Rampart Range thrust systems. These overlap southward with the Ute Pass–Cheyenne Mountain thrust system, which dies southward into the Canon City embayment.

On the western side of the range, Laramide geometries are overprinted by more extensive post-Laramide fault and igneous systems. Still, exposures of the large displacement, low-angle Elkhorn, Williams Range, and Never Summer thrust faults indicate they defined the western limit of the basement arch during Laramide deformation. Horizontal fault displacements of at least 10 km (6 mi) are documented where post-Laramide plutons bow the faults upward, forming tectonic windows exposing Cretaceous shales underneath Precambrian rocks of the Front Range hanging wall (Ulrich 1963; O'Neill 1981).

Vertical tectonic interpretations invoking dip slip on high-angle, range-bounding faults provided an integrated hypothesis for the Front Range (Fig. 2a; Boos and Boos 1957; Matthews and Work 1978) by explaining the low-angle faults as gravity slides. This interpretation has been questioned on the basis of the magnitude of the overhangs, the faults' consistency along strike, and their associated shortening structures. Symmetric, concave-downward upthrusts on the arch margins (Fig. 2b) were proposed by Prucha et al. (1965) and Jacob (1983) as a means to explain the observed horizontal shortening within a vertical tectonic framework.

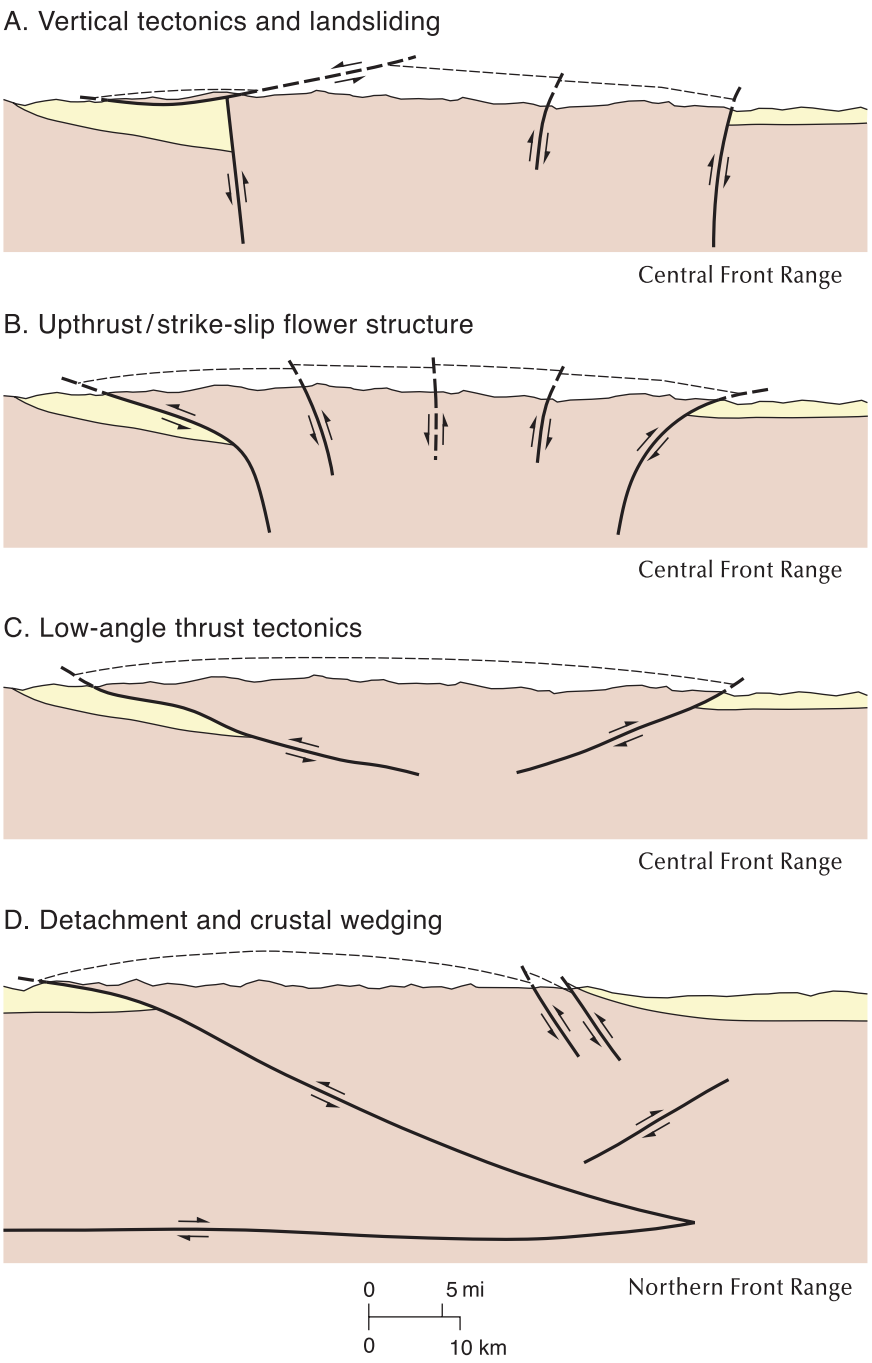

FIGURE 2—Simplified cross-sections of tectonic models for the Front Range based on (**a**) vertical uplift, with gravity sliding on western flank, (**b**) symmetric up-thrusts (Jacobs 1983) and positive strike-slip flower structures (Kelley and Chapin 1997), (**c**) low-angle, symmetric thrust faulting in the central Front Range (Raynolds 1997), and (**d**) backthrust basement wedge in the northern Front Range (Erslev and Holdaway 1999).

Hypotheses of strike-slip deformation have also been suggested, often using a cross-sectional geometry similar to that of the upthrust model but suggesting large amounts of strike slip on the bounding faults (Chapin 1983; Daniel et al. 1995; Kelley and Chapin 1997). Cather (1999b) provided a potential explanation for the similar strikes of proposed strike-slip and thrust systems by noting analogous patterns along major transform boundaries where the slip is partitioned into distinct thrust and strike-slip components.

Thrust models have also been proposed for the Front Range arch (Warner 1956). Raynolds (1997) used sedimentologic evidence for thrust loading on the flanks of the central Front Range to propose a symmetric thrust model (Fig. 2c) for the southern Front Range arch. Kluth and Nelson (1988) used the timing of the sediments to propose an asymmetrical development of these arch-bounding thrust faults, with major movement on western thrust faults tilting the arch to the east first, followed by the eastern thrust faults breaking through to the surface. Erslev (1993) and Holdaway (1998) showed that the northern Front Range arch can be modeled by an asymmetrical chip (Fig. 2d), where the northeastern flank of the arch is underthrust by a wedge of lower crust whose roof thrust defines the western side of the arch.

A. Northeast Front Range

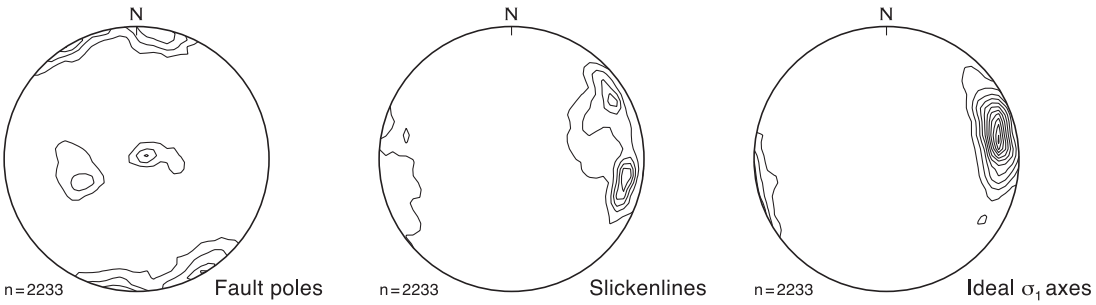

B. Eastern Front Range northwest of Denver

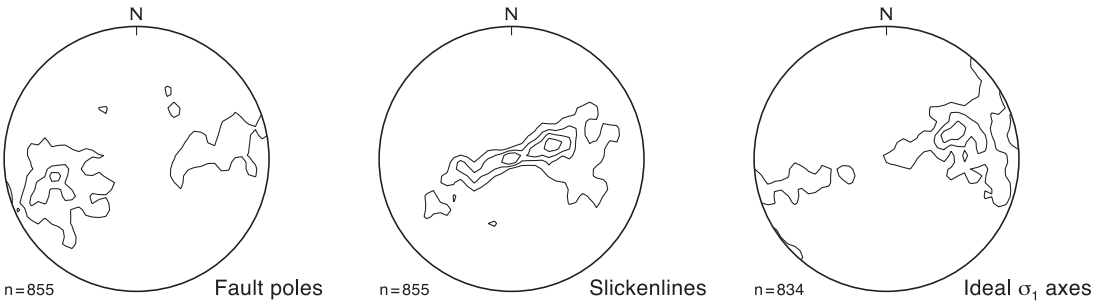

C. Canon City embayment

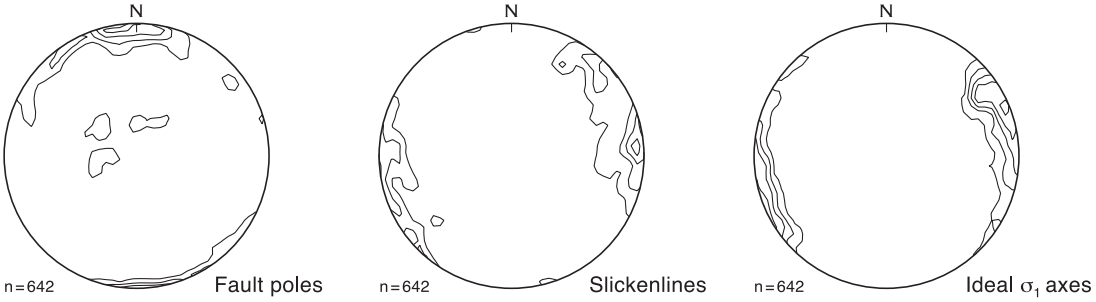

D. Webster Park, southern Front Range

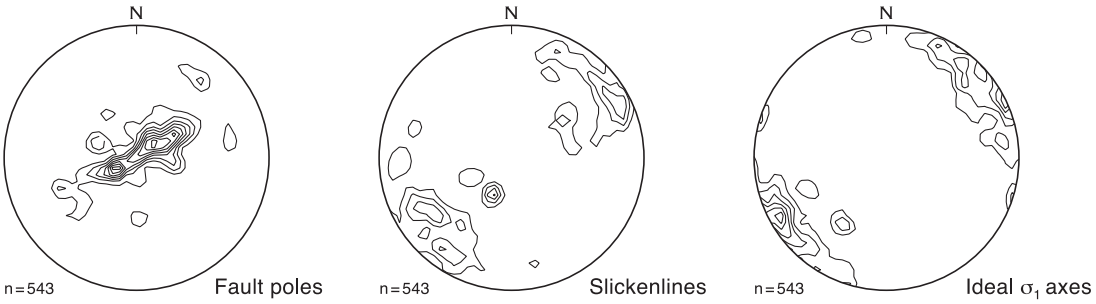

E. West-central Front Range

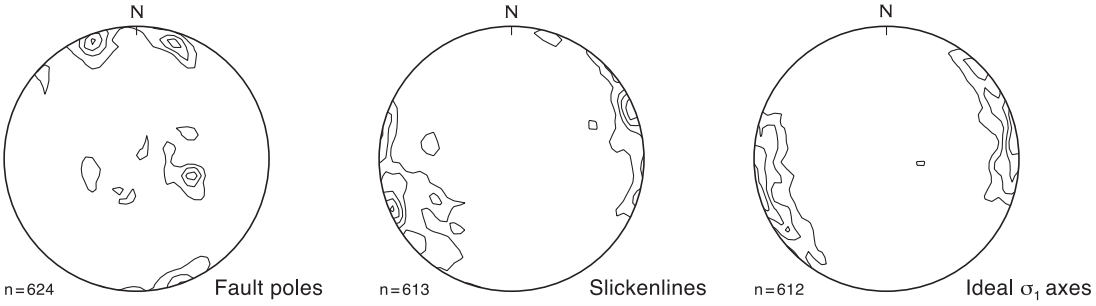

In addition, multi-stage models for Laramide deformation (e.g., Chapin and Cather 1981; Gries 1983) have suggested that the Laramide foreland may have developed sequentially about differently oriented stress and strain axes. Gries (1983) used structural geometries and sedimentary basin characteristics to propose a counterclockwise rotation of shortening and compression axes from east-west to north-south orientations during the Laramide. Chapin and Cather (1981) combined changes in dike orientations and sedimentary basin geometries in the Southern Rocky Mountains to predict an early east-northeast shortening event followed by a northeast shortening event dominated by right-lateral strike-slip faulting. Chapin (1983) further developed the hypothesis of Laramide right-lateral faulting along the eastern margin of the Colorado Plateau and suggested that a number of major north-striking faults in the Front Range may be dominated by strike-slip movement. Bird (1998) combined fault geometries, kinematic information and plate geometries to propose that the Southern Rocky Mountains may have undergone multi-phase, multi-directional compression related to the different convergence directions of the Farallon and Kula plates as they were subducted under North America. Unlike the counter-clockwise interpretations of Gries (1983) and Chapin and Cather (1981), however, Bird predicted clockwise rotation of compression and shortening directions through time.

Recent fault analyses in southwest Colorado (Erslev 1997; Ruf 2000) and northern New Mexico (Erslev 2001) have documented sequential, multi-directional shortening and compression using minor fault analyses. In southwest Colorado near Durango, multiple conjugate fault sets indicate that northeast shortening was followed by northwest shortening, and both were overprinted by post-Laramide north-northeast shortening and normal faulting (Ruf 2000). In northern New Mexico, clear cross-cutting relationships show a similar sequence, with faults indicating east-northeast and east-west shortening cut by faults indicating north-northeast shortening (Erslev 2001). At least some of the faults associated with late stage north-northeast shortening are post Laramide because they cut rocks as young as 24 Ma. Similar mid-Tertiary strike-slip faults have been reported from the southern Front Range at Cripple Creek (Wawrzyniec et al. 1999) and in eastern North Park (Erslev et al. 1999).

Each of these hypotheses predict different stress histories, which can be tested by minor fault analyses. Vertical tectonic hypotheses (Fig. 2a) predict a combination of high-angle dip-slip faults and lower-angle normal faults resulting from gravitational collapse of the range. Upthrust hypotheses (Fig. 2b) predict a range of high- to low-angle dip-slip faulting. Strike-slip hypotheses (Fig. 2b) suggest that at least some of the minor faults paralleling the major faults should be dominated by strike slip. If slip is partitioned between thrust and strike-slip systems, one might also expect to see stress and strain refraction patterns adjacent to major strike-slip faults. Thrust hypotheses (Figs. 2c,d) predict shortening and compression axes oriented perpendicular to the strike of major faults and a lack slip parallel to the strike of these faults. Multi-stage, multi-directional hypotheses suggest that Laramide fault patterns should reveal regionally-consistent multi-modal distributions of shortening and compression directions.

FIGURE 3—Contoured stereonet plots of poles to faults, slickenlines and ideal σ_1 axes (Compton 1966) for each area. The plots are contoured using the Schmidt method (Vollmer 1992), with a 2% contour interval calculated over 40 nodes.

Minor fault analysis methods

Slickensided minor fault surfaces were measured within five areas (Fig. 1) along the flanks of the Colorado Front Range (see the appendix for individual locality data). Because this research focused on Laramide faulting, faults at localities of Pennsylvanian and older rocks were avoided because of the possible presence of faults related to the Ancestral Rocky Mountain and Precambrian orogenies. Similarly, localities exposing rocks younger than 40 Ma were not analyzed in detail by this paper because they are presumed to record post-Laramide faulting, which was not the focus of this study.

In general, faults with the best-preserved slickenside lineations were found in silica-cemented quartz arenites, which are common in the Cretaceous Dakota, Jurassic Morrison, and Permian Ingleside Formations. In general, slickenlines within major fault zones were rarely observed because of poor exposures and pervasive cataclasis. Because more highly folded strata have complex slickenline orientations caused by the added complexities of fold-related slip (e.g., flexural slip) and rotation of early-formed slickenlines, wherever possible this study concentrated on localities with strata dipping less than 35°.

At each outcrop, slickenside strike and dip were measured as well as slickenline trend, plunge, and shear sense. Shear sense was determined using the criteria of Petit (1987) with most fault planes displaying excellent Riedel fractures and some containing calcite growth fibers. In this area, minor faults commonly form conjugate sets, with acute bisecting angles between conjugate faults ranging from 60° to 30°. Acute bisectors of conjugate strike-slip and thrust faults commonly parallel bedding with the resulting discordance of most faults to bedding ensuring that they did not reactivate pre-existing bedding weaknesses.

Where possible, approximately 20 fault surfaces were measured for each fault set indicating horizontal shortening. The possibility of multiple fault sets was considered where faults did not conform to simple conjugate patterns. A key to deducing the relative ages of conjugate fault sets is the cross-cutting relationships between fractures which belong to only one conjugate set. In addition overprinting of slickenlines on individual fault surfaces can give timing relationships. Where cross-cutting and overprinting relationships are not evident, the chronology of fault slip can be estimated by the more complete preservation of the latest slickenlines.

Fault data for each area is presented in stereonets which plot fault plane pole, slickenline and ideal σ_1 axis (Compton 1966) orientations (Fig. 3). In addition, smoothed rose diagrams of slickenline and ideal σ_1 axis trends are plotted in Figure 4 to provide a graphical portrayal of their angular distribution and to identify multiple modes of slip and ideal compression directions. Rose diagrams presented in this paper are smoothed to clarify their interpretation, with the petal length for each 1° increment proportional to the number of slickenlines within 5° of each increment. Rose diagrams from north-central New Mexico (Fig. 4f) are provided as an example of multi-stage, multi-directional faulting with which to compare the Front Range data. The multi-stage nature of faulting in this area of New Mexico is confirmed by cross-cutting relationships. For instance, the north-south strike-slip faults cut post-Laramide strata as young as 24 Ma (Erslev 2001).

In areas where conjugate shear bands without slickenlines are the only available faults, shear band strikes and dips were used to estimate the orientation of the σ_1 axis for each locality. The average orientation of each conjugate was calculated by eigenvector analysis and then used to find the

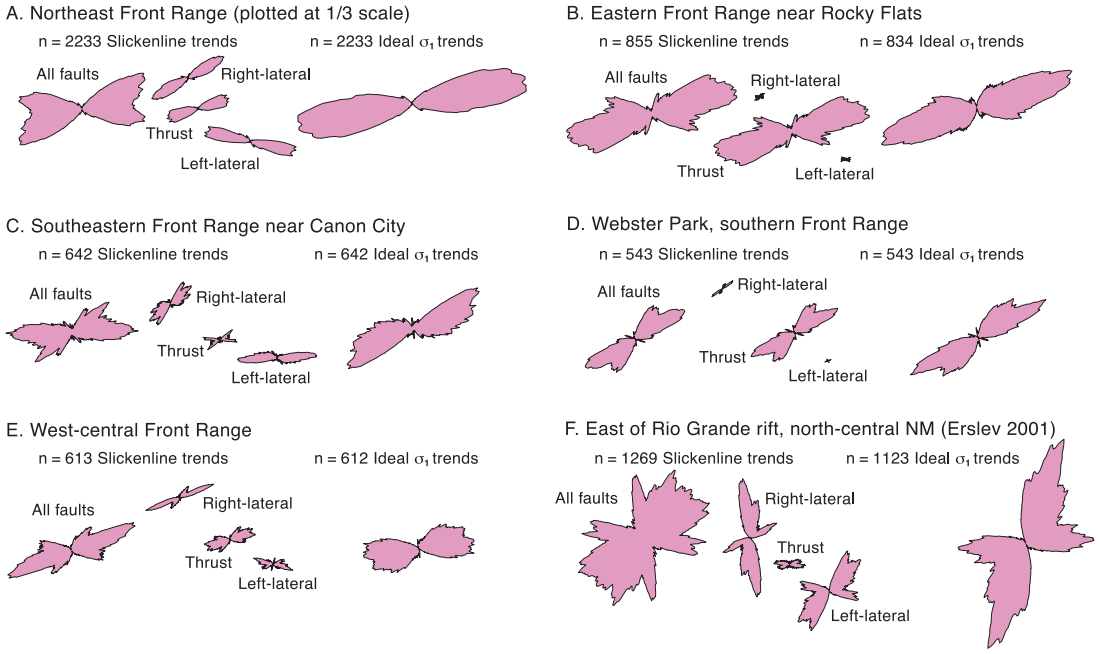

FIGURE 4—Rose diagrams of minor fault slickenline trends, both composite and separated by fault type, and ideal σ_1 axis trends for Front Range localities and north-central New Mexico (Erslev 2001, included here for comparison). Rose diagrams are smoothed by plotting the number of trends within 5° of each 1° increment. In general, lineations with plunges greater than 45° are not included in the rose diagrams with the exception of those from the eastern Front Range near Rocky Flats.

acute bisector of the conjugate pair, which is assumed to parallel the σ_1 axis. Comparisons of conjugate acute bisectors with ideal σ_1 axes for localities with slickensided faults show that they are highly correlative (Fryer 1997).

Although the most direct interpretation of slickensided faults is as strain, the summation of a total strain from minor faults requires knowledge of the amount of slip on each fault. Unfortunately, net slip could be estimated for only a very small fraction of the faults. This is particularly true for strike-slip faults, whose bedding-parallel slip is difficult to measure. In addition, the lack of slip data for larger, gouge-filled faults casts doubt on the regional validity of any strain value derived from the smaller slickensided faults.

Consequently, this paper attempts to quantify minor fault data in terms of average slickenline and ideal σ_1 axis (Compton 1966) orientations, which parallel the acute bisectors of conjugate faults. Average slip directions are given by the orientation of the first eigenvector of the slickenline trends and plunges (Table 1). The degree of clustering is given by the associated eigenvalue (E_1), where $E_1 = 1.0$ indicates perfect clustering about one orientation and $E_1 = 0.33$ indicates the absence of a single preferred orientation.

The trend of slickenlines varies with fault type. In the relatively simple, unidirectional faulting in the northeast Front Range of Colorado (Fig. 4a; Erslev and Selvig 1997; Holdaway 1998) right-lateral, thrust, and left-lateral faults form unimodal distributions, which can be combined into a trimodal rose diagram representing all fault slip trends. This trimodal spread of slickenline trends complicates their use for discrimination of multiple shortening and compression directions.

For simple conjugate faulting, the spread in trend orientations is largely eliminated by plotting ideal σ_1 axes, which are assumed to parallel the acute bisector of the conjugate sets. This technique was used by Compton (1966), who determined ideal σ_1 axes by moving half the bisector angle (2σ) from the slickenline towards the direction of maximum compression within the plane containing the pole to the fault and the slickenline. For this paper, an σ angle of 25°, consistent with Byerlee (1978), was used by our SELECT program to calculate the ideal σ_1 axis for each fault. Because most of the fault sets are symmetrically weighted, with equal numbers of right- and left-lateral faults, and equal numbers of thrust conjugates, small changes in σ angles cause less than 5° of change in average σ_1 axis orientations. These ideal stress calculations assume fracture on ideal conjugate planes, an assumption which is violated by reactivated fault planes and some cases of three-dimensional strain.

Additional methods for determining stress and strain axes are presented in the theses of Selvig (1994), Jurista (1996), Fryer (1997), and Holdaway (1998) and these will be compared in a future paper. The ideal σ_1 axis technique has advantages over the Angelier (1990) least-squares algorithm, which uses fault slip directions to calculate a reduced stress tensor, in that outlying measurements do not have a large influence on stress directions. For the case of fault data from the eastern and southern Front Range of Colorado (Jurista 1996; Fryer 1997; Erslev and Selvig 1997; Holdaway

TABLE 1—Average slickenline and ideal σ_1 axes for the Front Range, showing average trend, plunge and eigenvalue ($\mathbf{E_1}$). **n** = number of measurements.

		Slickenline		Ideal σ_1 axes	
Location	**n**	**trend-plunge**	**E_1**	**trend-plunge**	**E_1**
Northeast Front Range	2233	080-13	0.7232	079-11	0.8397
Eastern Front Range	834	087-66	0.5513	075-25	0.5735
Canon City embayment	642	076-06	0.6697	075-04	0.7393
Webster Park area	543	231-06	0.6416	233-01	0.7635
Western Front Range	612	250-06	0.6485	253-02	0.7189

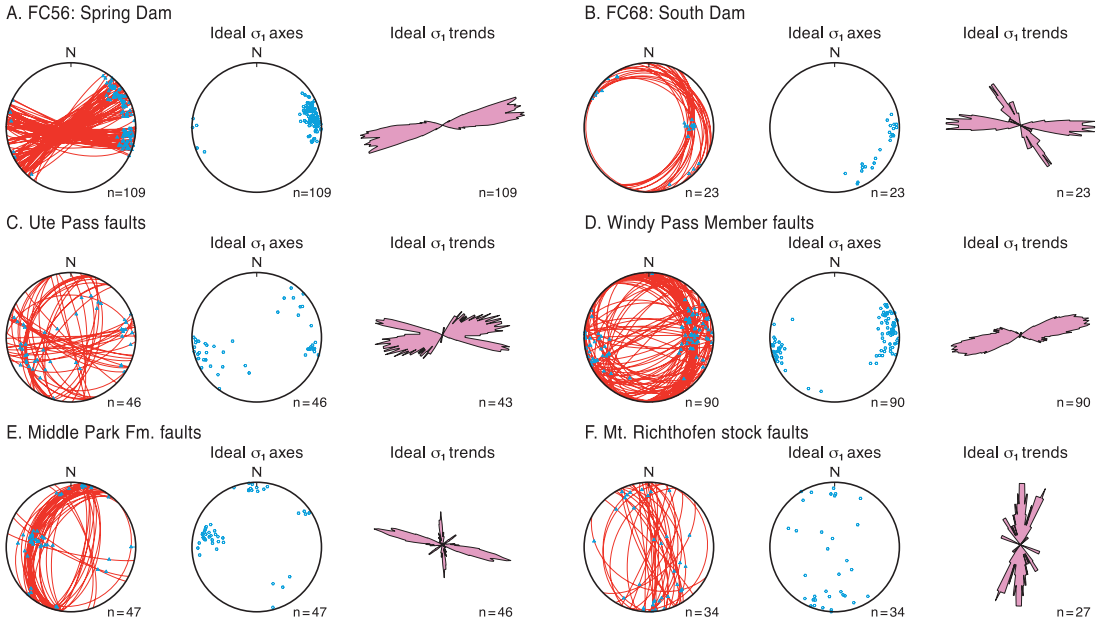

FIGURE 5—Stereonets of slickensided fault planes (plotted as arcs) with slickenside lineations (plotted as points), stereonets of ideal σ_1 axes, and smoothed rose diagrams of ideal σ_1 axis trends for individual localities from the northeastern (**A,B**) and west-central (**C–F**) Front Range

1998), the ideal σ_1 method gives higher precision (reproducibility) than the Angelier (1990) method. In addition, the ideal σ_1 method aids in separation of faults into subsets with consistent σ_1 trends because faults are analyzed individually. By plotting ideal σ_1 axes and analyzing their variability with rose diagrams and eigenvector analyses, data are portrayed in a format allowing relatively unbiased evaluation of the possibility of multiple directions of shortening and compression.

Minor fault analyses

The fault orientations and their ideal σ_1 axis trends are presented as contoured stereonets (Fig. 3), rose diagrams (Fig. 4), average orientations (Table 1), locality data (Appendix), and data from selected individual localities (Fig. 5). These orientations are sufficient to eliminate vertical tectonic models from consideration. Whereas fault plane orientations are quite variable from area to area, the slickenlines and their ideal σ_1 axes strongly indicate subhorizontal slip and compression. The one exception is the high-angle slickenlines from the eastern Front Range northwest of Denver. This data set is dominated by data from highly rotated strata in the famous flatirons south of Boulder.

Further interpretation of the faults requires the examination of the detailed setting of the data. This section will start with a description of the northeast Front Range near Fort Collins, for which we have the largest and simplest data sets, and move to the south and west before ending with a description of the west-central Front Range, which has the most complicated data sets.

Northeastern Front Range

The eastern flank of the Front Range exposes a diverse set of structures, with the major, north-northwest-striking fault systems west and south of Denver bringing the crystalline rocks of the core of the Front Range up relative to the Denver Basin. However, to the north, a series of north-northwest-striking, en echelon faults transect the north-trending boundary of the range and bring the eastern basin side of the faults up relative to the western, arch side of the faults (Figs. 6–9).

These basement-involved faults are overlain by fault-propagation folds, which progressively transform the faulting into folding of the sedimentary cover (Erslev and Rogers 1993). Dip and slip-sense interpretations of the major faults have varied dramatically through the years. Ziegler (1917) proposed motion on planar reverse and thrust faults, predicting that a 50° dipping reverse fault underlies Milner Mountain anticline (Fig. 8), the only fault large enough to actually cut through the Cretaceous Dakota Group. Boos and Boos (1957) also showed a planar reverse fault in an analogous section but steepened the fault dip to around 80°. Prucha et al. (1965) introduced the concept of concave downward upthrusts to the area. By increasing fault dips downward, from 30° dipping thrusts in the sedimentary strata to vertical faults cutting basement, lower angle thrust faults in the cover were explained within a vertical tectonic framework. This upthrust geometry was adopted by Braddock et al. (1970) and Le Masurier (1970) for Milner Mountain anticline, which they interpreted as being underlain by a 60° dipping reverse fault that becomes vertical at depth. A further evolution of fault dip interpretations was contributed by Matthews and Work (1978) who suggested that a planar normal fault with a dip of 80° underlies Milner Mountain anticline.

The vertical tectonic interpretations of these structures are in clear conflict with the evidence for horizontal shortening and compression in the Rocky Mountain foreland. Recent work at Colorado State University (Erslev and Rogers 1993; Erslev 1993; Selvig 1994; Holdaway 1998) has shown that major fault dips in the Fort Collins area range from 20° to 70° to the northeast, consistent with the early interpretations of Ziegler (1917). These angles of faulting are compatible with the lateral contraction indicated by seismic information to the north (Laramie Range: Brewer et al. 1982; Johnson and Smithson 1985) and south (Golden Fault: Jacob 1983; DOE 1993; Erslev and Selvig 1997; Weimer and Ray 1997), which indicate large, west-dipping thrust faults overlapping the western margin of the Denver Basin.

Curiously enough, the thrust and reverse faults in the northeastern Front Range cannot be directly responsible for

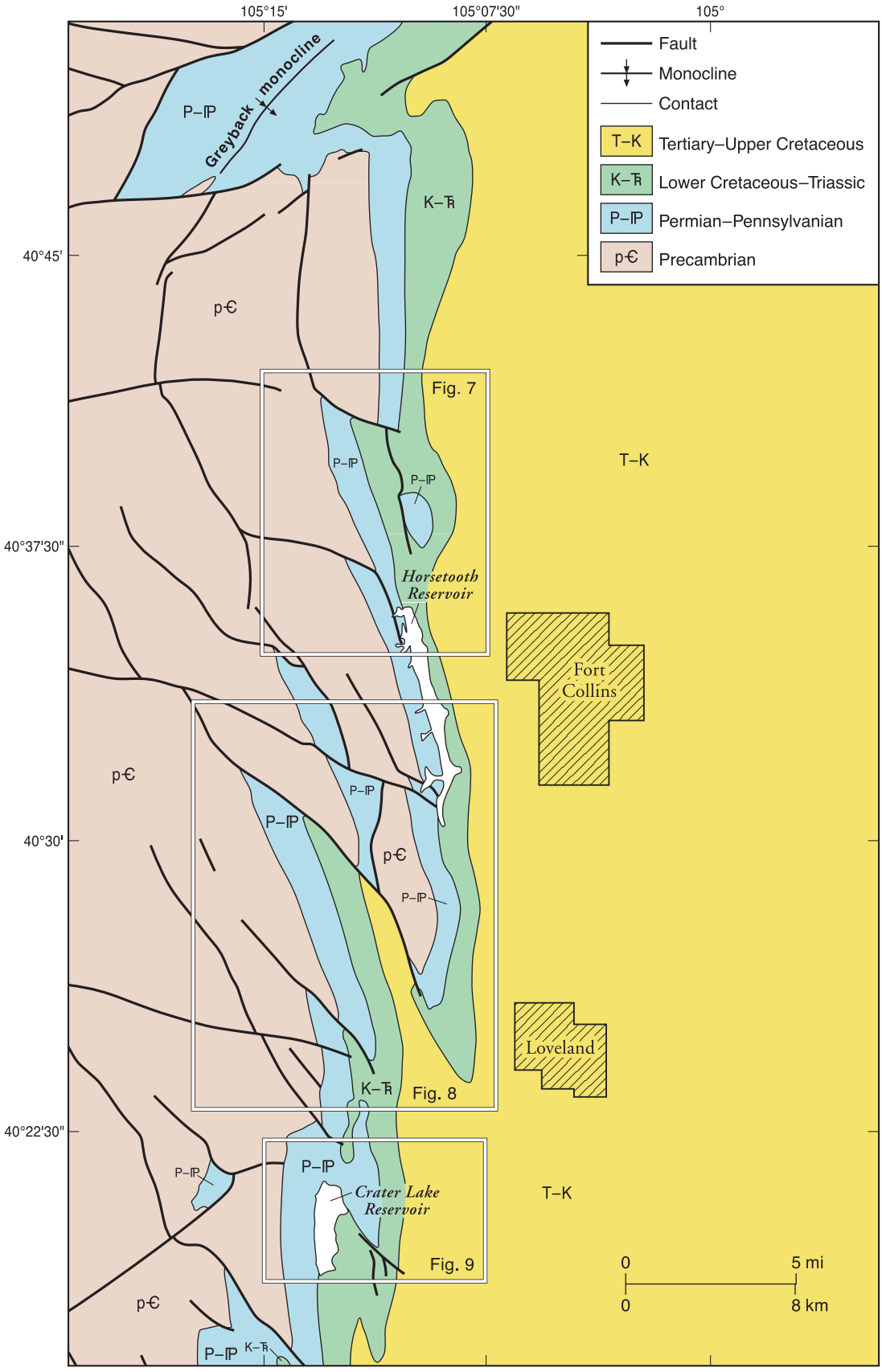

FIGURE 6—Simplified geologic map of the northeastern Front Range (after Tweto 1979) outlining the location of more detailed maps in subsequent figures.

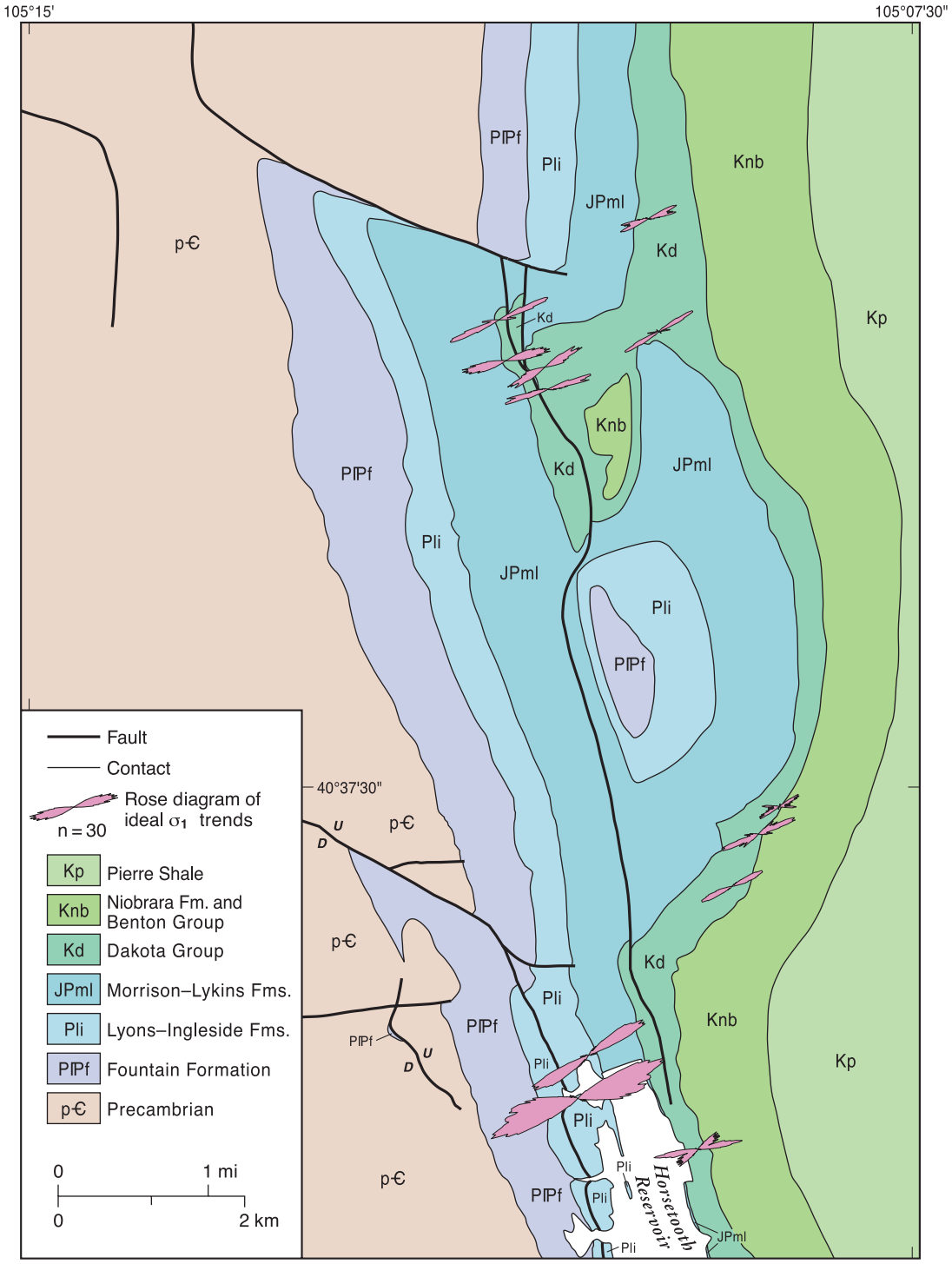

FIGURE 7—Simplified geologic map (after Braddock et al. 1988a, 1989) of the eastern margin of the Front Range northwest of Fort Collins, Colorado. Smoothed rose diagrams show the trends of ideal σ_1 axis trends from individual outcrops (Holdaway 1998).

the uplift of the range because their northeasterly dip brings the basin up relative to the range. These faults were explained by Erslev and Selvig (1997) as second-order backthrusts off a blind, east-northeast-directed thrust in the basement. More recent work by Holdaway (1998) has shown that an additional component of deep crustal wedging is necessary to uplift the range (Fig. 2d). In this case, thrusts on the northeastern flank of the Front Range probably formed due to synclinal tightening during wedging at depth analogous to structures on the northeast side of the Wind River Mountains (Erslev 1986). This back-limb tightening hypothesis (Stanton and Erslev 2001) is consistent with the asymmetrical uplift of the arch previously proposed by Kluth and Nelson (1988).

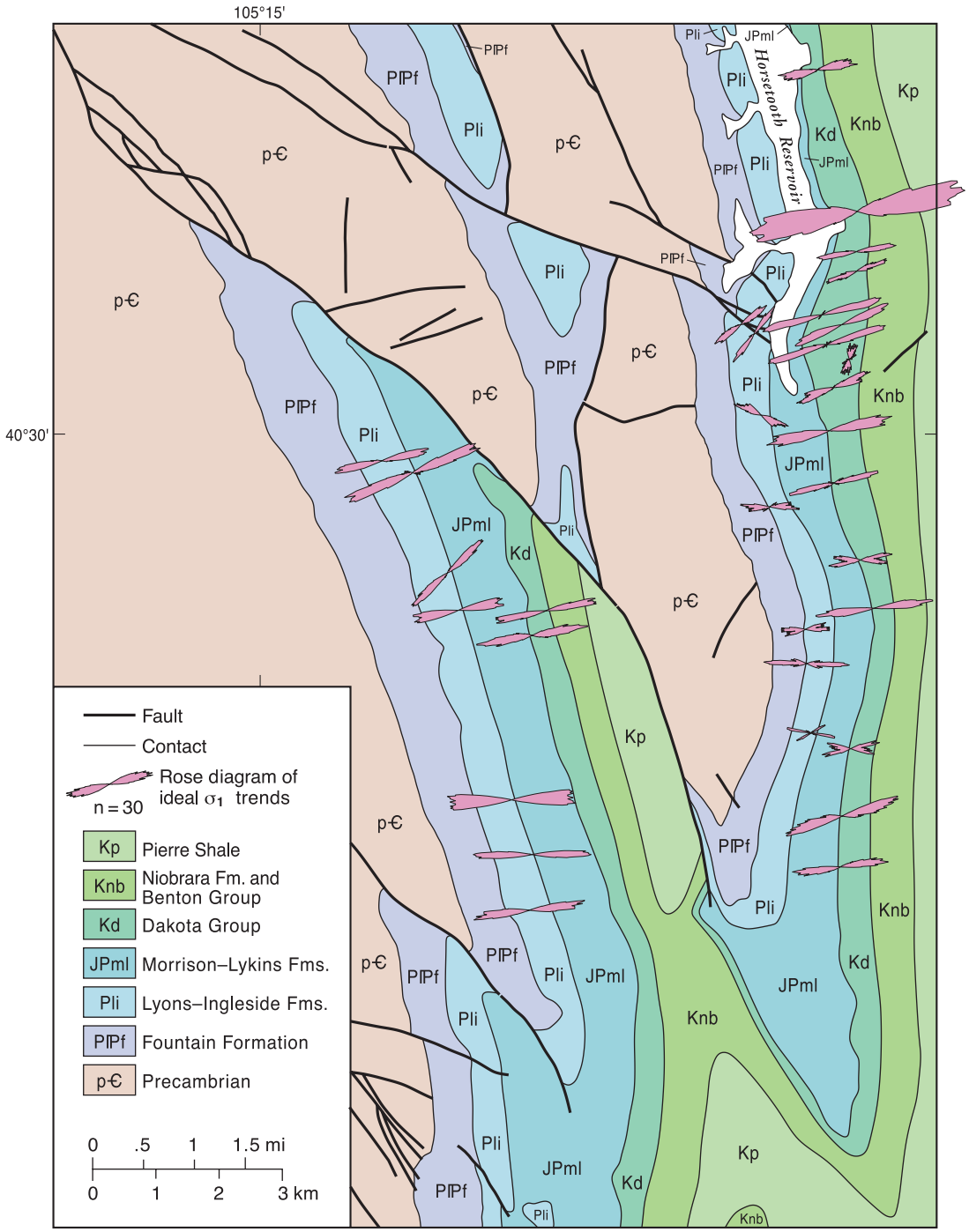

FIGURE 8—Simplified geologic map (after Braddock et al. 1970, 1989) of the eastern margin of the Front Range west of Fort Collins, Colorado. Smoothed rose diagrams show the trends of maximum compression directions from individual outcrops from Holdaway (1998).

Minor faults confirm the importance of horizontal compression and shortening in the northeastern Front Range. Stereonets of fault plane and slickenline orientations (Fig. 3a) form 4 modes consistent with two conjugate sets, one thrust set and one strike-slip set. These share a common ideal σ_1 direction with an average orientation of N79°E-11 (trend-plunge). This shortening and compression direction also is evident in rose diagrams of slickenline and ideal σ_1 trends (Fig. 4a). Individual localities most commonly show conjugate faulting about a single ideal σ_1 direction (e.g., Fig. 5a). Two localities show bimodal distributions that are not due to reactivation of pre-existing weaknesses and are hard to attribute to local structural complications (e.g., Fig. 5b). At both of these localities, thrust slickenlines indicating northwest-southeast shortening and compression overprint slickenlines indicating more east-west shortening and compression.

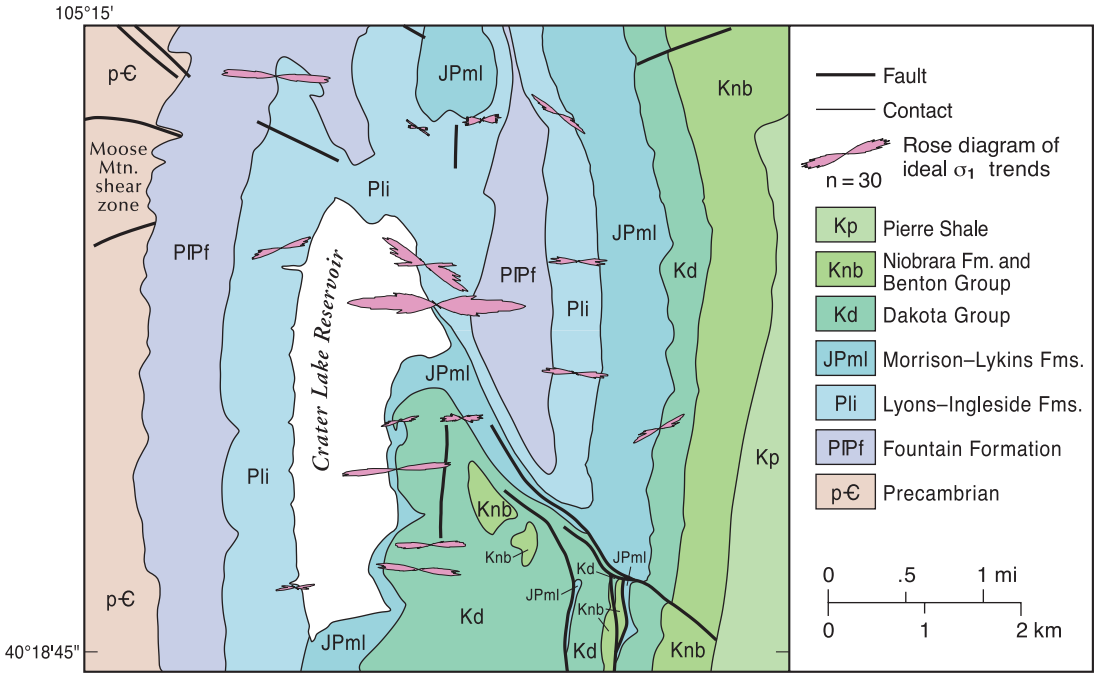

FIGURE 9—Simplified geologic map (after Braddock et al. 1988b) of the eastern margin of the Front Range southwest of Fort Collins, Colorado. Smoothed rose diagrams show the trends of maximum compression directions from individual outcrops from Holdaway (1998).

Rose diagrams of ideal σ_1 axis trends for individual localities plotted on geologic maps (Fig. 6–9) show little discernable influence of the local structures, with rose diagrams showing an east-northeast orientation regardless of bedding strike. In a few places, rose diagrams indicate that ideal σ_1 axis trends immediately adjacent to major faults deviate from the average trends and instead are arrayed nearly perpendicular to the faults. On a regional scale, however, there is a correlation between the average orientation of the range front and the average trend direction. West of Fort Collins (Figs. 7, 8), where the average basement unconformity strikes N20°W, the average ideal σ_1 direction trends N72°E. In contrast, in the area near Carter Lake (Fig. 9) where the average basement unconformity strikes due north-south, the average ideal σ_1 direction trends S86°E.

The nature of the major faults is clear from the orientations of the rose diagrams of slickenline trends from individual fault types. Strike-slip slickenline trends (Fig. 4a) do not parallel the major faults, suggesting minimal strike slip on these major faults. The dip directions of the largest faults in the area (e.g., the Milner Mountain and Redstone Creek faults) are parallel to the thrust fault dip directions and the average ideal σ_1 directions, again indicating a dominance of thrust movement over strike-slip movement. The dip directions of several of the other major faults are more northeasterly than the average east-northeast σ_1 orientations, suggesting a slight left-lateral slip component on these faults. Left-lateral slip cannot be a major component of the slip, however, because all of these faults generated right-lateral separations on the basement unconformity.

Eastern Front Range northwest of Denver

An intriguing structural transition is present in the eastern margin of the Front Range west of Denver. South of Boulder, the east-tilted hogbacks characteristic of the northeastern range margin steepen, as do the east-dipping en echelon faults which transect them (Figs. 1, 10). South of the Rocky Flats plant, a deactivated nuclear weapons plant, the west-dipping Golden fault system brings the Precambrian basement up and over the sedimentary strata of the Denver Basin. This thrust system is complicated, with recent structural balancing by Sterne (1999) indicating that it is a complex triangle zone.

A seismic line through the Rocky Flats plant crossed the mountain front and revealed both exposed and blind splays of the Golden fault system (DOE 1993; Erslev and Selvig 1997; Weimer and Ray 1997). Balancing arguments indicate that displacement on these west-dipping thrust faults must be transferred to the east-dipping backthrusts, which segment the flat irons south of Boulder (Selvig 1994). Erslev and Selvig (1997) suggested that the west-dipping thrusts of the Golden fault system diverge in this area forming a broad zone of shear that tilted the flat irons toward the Denver basin by domino-style backthrusting.

The area near the Rocky Flats plant is further complicated by its intersection with the Wattenberg high. This feature has many low-angle thrust faults which strike northeast and repeat Cretaceous and Paleogene strata (Kittleson 1992). The Wattenberg high is an area of uplift centered on a massive, northeast-trending thermal anomaly paralleling a band of Laramide intrusions to the southwest along the Colorado Mineral Belt. The anomalous northeast-striking thrust faults may be because of gravity collapse of the sedimentary cover off the Wattenburg high into the center of the Denver Basin to the southeast, perhaps aided by thermal maturation of hydrocarbons during heating of the Wattenberg high (Erslev and Selvig 1997).

Minor faults in the area of the range front near Rocky Flats plant (Fig. 3b) have an important but complicated history. Because of the scarcity of low-dipping beds with slickensided faults in the area (see appendix for bed and average fault attitudes at each locality), trends greater than 45° have not been culled from the data set plotted in Fig. 4b. In addition, the individual rose diagrams in Figure 10 have been

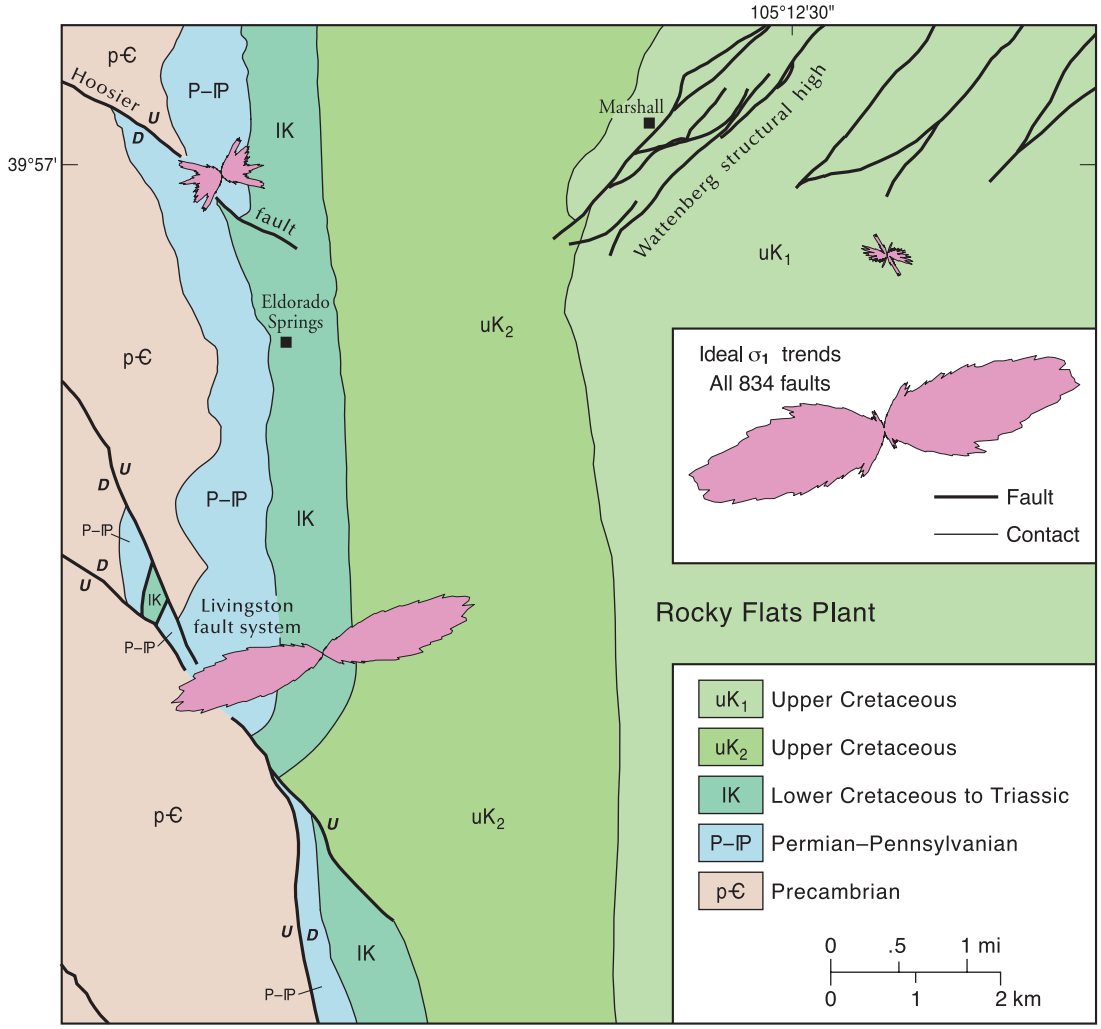

FIGURE 10— Simplified geologic map of the eastern margin of the Front Range south of Boulder. Smoothed rose diagrams show the trends of ideal σ_1 axis trends for three major domains from Selvig (1994).

plotted for domains, not individual localities, because of the complexity of the data set and the need for broader averaging of the data.

Fault poles (Fig. 3b) show the dominance of high-angle reverse faults, often approximately paralleling the rotated bedding orientation. Slickenlines show a diffuse, near vertical maximum elongated in an east-northeast–west-southwest direction. Ideal σ_1 axes are more horizontal, but again are distributed about an east-northeast–west-southwest direction. Rose diagrams showing distribution by fault type show the overwhelming predominance of dip-slip thrust and normal faults, which probably represent rotated thrust faults. Rose diagrams for the Hoosier and Livingston domains along the range front (Fig. 10) show ideal σ_1 axis trends similar to those in the northeastern Front Range. Their oblique orientation to both the Hoosier and Livingston backthrusts as well as the north-south range front suggests slip oblique to both structural elements.

A minor, distributed mode of east-southeast-trending slickenlines and ideal σ_1 axes (Figs. 3b, 4b) is contributed by faults on the flank of the Wattenburg structural high (see small rose diagram in northeast corner of Fig. 10). Selvig (1994) attributed these to gravity sliding because there is no evidence that they are rooted below the Upper Cretaceous strata.

Southern Front Range

The southern Front Range arch plunges southward into the Canon City embayment where it disappears. Slip is presumably taken up on the southeast-plunging Wet Mountain arch, whose relief also dissipates to the south. Tweto (1980) used unconformities and sedimentary rock distributions to show that the Front Range, Wet Mountain, and southern Sangre de Cristo arches were uplifted in the Pennsylvanian by the Ancestral Rocky Mountain orogeny (DeVoto 1980; Tweto 1980; Kluth and Coney 1981). As a result, these ranges were extensively eroded and then covered by Jurassic and Cretaceous sediments before Laramide deformation.

Laramide uplift of the Wet Mountains and Front Range was initiated in the Late Cretaceous, as indicated by synorogenic sediments deposited on their flanks (Tweto 1975; Kluth and Nelson 1988). Laramide uplift ended in early Tertiary time, and the area formed an extensive late Eocene erosion surface, which truncates Laramide structures (Epis and Chapin 1975; Leonard and Langford 1994).

The Wet Mountain arch is bounded by northwest-striking thrust faults on its eastern margin (Burbank and Goddard 1937; Logan 1966). A similarly-striking, anastomosing network of connected faults, the Ilse fault system, is found in the central region of the Wet Mountain arch. The Ilse fault and other northwest-striking faults that comprise the fault

system extend from the southern end of the Wet Mountains northward into central Colorado.

The Ilse fault system is bound by Precambrian rocks along most of the system's trace. In the northern Wet Mountains west of Canon City and the Royal Gorge area, however, the Ilse fault is bordered to the east by two sedimentary inliers at Webster Park and Twelvemile Park. The two inliers are separated from the Canon City embayment to the east by Precambrian crystalline rock of the south-plunging Royal Gorge anticline. The inliers themselves are separated by Precambrian crystalline rock exposures and are connected by the Ilse fault system, the northeast-striking Mikesell Gulch fault, and several north- to northeast-striking faults.

Lovering and Goddard (1938) compared the northwest-striking faults of the Wet Mountain arch to similarly-striking faults bounding the Front Range arch to the east and concluded that these faults were formed by east- or northeast-trending horizontal compression. In northern Webster Park, near the town of Parkdale, Johnston (1953) used fault and slickenline attitudes to infer an east to northeast Laramide compression direction.

In contrast, Chapin (1983) noted that wide zones of crushed and sheared rocks adjacent to the Ilse fault are similar to those adjacent to strike-slip faults. He proposed that the Ilse fault is a right-lateral strike-slip fault. But lateral separations of Precambrian rocks adjacent to the Ilse fault system do not support large-scale right-lateral slip. In the southern Wet Mountains, the Ilse Fault system cuts through the Precambrian San Isabel pluton with no obvious strike-slip separation. North of Webster Park, Taylor et al. (1975) mapped right-lateral separations of Precambrian rocks but these separations are only approximately 1.5 km. Approximately 3–8 km north of Twelvemile Park, the geologic map of Wobus et al. (1979) shows either no lateral separations or minor left-lateral separations.

Chapin and Cather (1981) documented the existence of narrow, elongate axial basins filled with Eocene clastic rocks along the eastern margin of the Colorado Plateau. Several of these basins, which they called Echo Park type-basins, have no Upper Cretaceous or Paleocene strata and thus appear to have been initiated in the Eocene, late in the Laramide orogeny. Echo Park, Chapin and Cather's type axial basin, lies approximately 13 km west of Webster Park and Twelvemile Park and the Ilse fault system. On the east side of the Echo Park Basin, Chapin and Cather (1983) noted a major shear zone containing highly sheared Precambrian rocks and, at several localities, slivers of Jurassic Morrison and Cretaceous Dakota Sandstone. Chapin and Cather (1981) noted that Echo Park-type basins have numerous similarities to wrench fault basins and proposed that these basins formed by a combination of horizontal shortening and right-lateral shear.

Unfortunately, slickensided minor faults were not found in the Eocene strata at Echo Park, probably because of a lack of sufficient cementation at the time of faulting. A small number of striated minor faults in the adjoining basement rocks yielded an average slip direction of S64°W-38 and an average ideal σ_1 axis oriented S61°W-24 (Fryer 1997). The interpreted slip direction and ideal σ_1 trend estimates are consistent with right-lateral oblique-slip. Unfortunately, because these minor faults were measured in Precambrian rocks, they may not represent Laramide deformation.

Extensive minor fault measurements were made around the margin of the Canon City embayment (Fig. 11; Jurista 1996) and east of the Ilse fault at Webster and Twelvemile parks (Fig. 12; Fryer 1997). For the Canon City embayment, stereonets and rose diagrams of fault poles and slickenline lineations (Figs. 3c, 4c) show that the area is dominated by right- and left-lateral faults, with a lesser number of thrust faults. Rose diagrams of the thrust and right-lateral faults are multi-modal, suggesting multiple directions of shortening and compression. The left lateral and ideal σ_1 axis distributions are more unimodal, although their rose diagrams show a marked asymmetry with a strong mode (N60°E for ideal v axis trends) and more trends clockwise of the main mode than in the counterclockwise direction.

Whereas the multi-modal rose diagrams suggest multidirectional faulting, individual locality information (Fig. 11) does not show consistent multi-modal pattern around the Canon City embayment. The asymmetrical distribution of ideal σ_1 axis trends is more consistent with variable influences of localized stresses. In several locations where beds are oblique to the average N30°W trend (e.g., locations plotted in Figure 11 south of Fort Carson Military Reservation and immediately south of Wetmore), oblique ideal σ_1 axis trends suggest local control of fault slip patterns.

To the west of the Canon City embayment at Webster and Twelve Mile parks (Fig. 12), faults are dominantly thrusts (Figs. 3d, 4d). For the large number (approximately 75% of the faults measured, see Fryer 1997 for details) of unslickensided faults, average conjugate bisectors are shown as arrows in Figure 12. Again, thrust fault slickenline and ideal σ_1 axis trends (Fig. 4d) do not yield a simple, symmetric mode of orientations. The dominant N60°E mode is nearly identical to that from the Canon City embayment. Unlike the faults around the embayment, however, the secondary distribution of ideal σ_1 axis trends are rotated clockwise relative to primary mode.

Individual locality data at Webster and Twelve Mile parks also show a lack of consistent multi-modal patterns, although distinctly different ideal σ_1 axis trends can be discerned. Ideal σ_1 axis trends that deviate from the main N60°E mode are most common at localities within 1 km of the northeast-striking Mikesell Gulch and east-striking Gorge faults. In addition, three localities with multiple conjugate fault sets are within 1 km of these map-scale faults, suggesting localized deviations in the strain and stress field. Separations on these major faults, and their strikes relative to those of strike-slip minor faults, suggest that the Mikesell Gulch fault is right lateral and the Gorge fault is left lateral. The faults may have provided local stress releases, causing localized stress refraction resulting ideal σ_1 axis trends that vary from the regional trend.

West-central Front Range

The western side of the Front Range is bounded by two basins, South Park Basin and Middle–North Park Basin, which probably represent the remnants of a once continuous thrust-bounded axial basin. The bounding faults are the largest in the region. The Elkhorn fault extends northward along the eastern margin of South Park until it appears to merge with the Williams Range thrust at the northern-most tip of South Park (Bryant et al. 1981). The Williams Range thrust extends northward along the eastern boundary of Middle Park towards Kremmling. The en echelon Never Summer thrust steps east from the Williams Range thrust north of Kremmling where it defines the east side of North Park.

The onset of faulting on the west side of the Front Range is regarded to be marked by the age of the 70 Ma Pando Porphyry near Minturn, about 30 km to the west (Tweto and Lovering 1977). Synorogenic Paleocene units are overridden by the Elkhorn thrust in South Park and by the Never Summer thrust in North Park (O'Neill 1981), indicating that thrusting continued into early Eocene. Unlike the higher angle reverse faults of the eastern margin of the Front Range, thrusts on the west side of the range commonly have low angle to nearly horizontal dips. Displacements on these

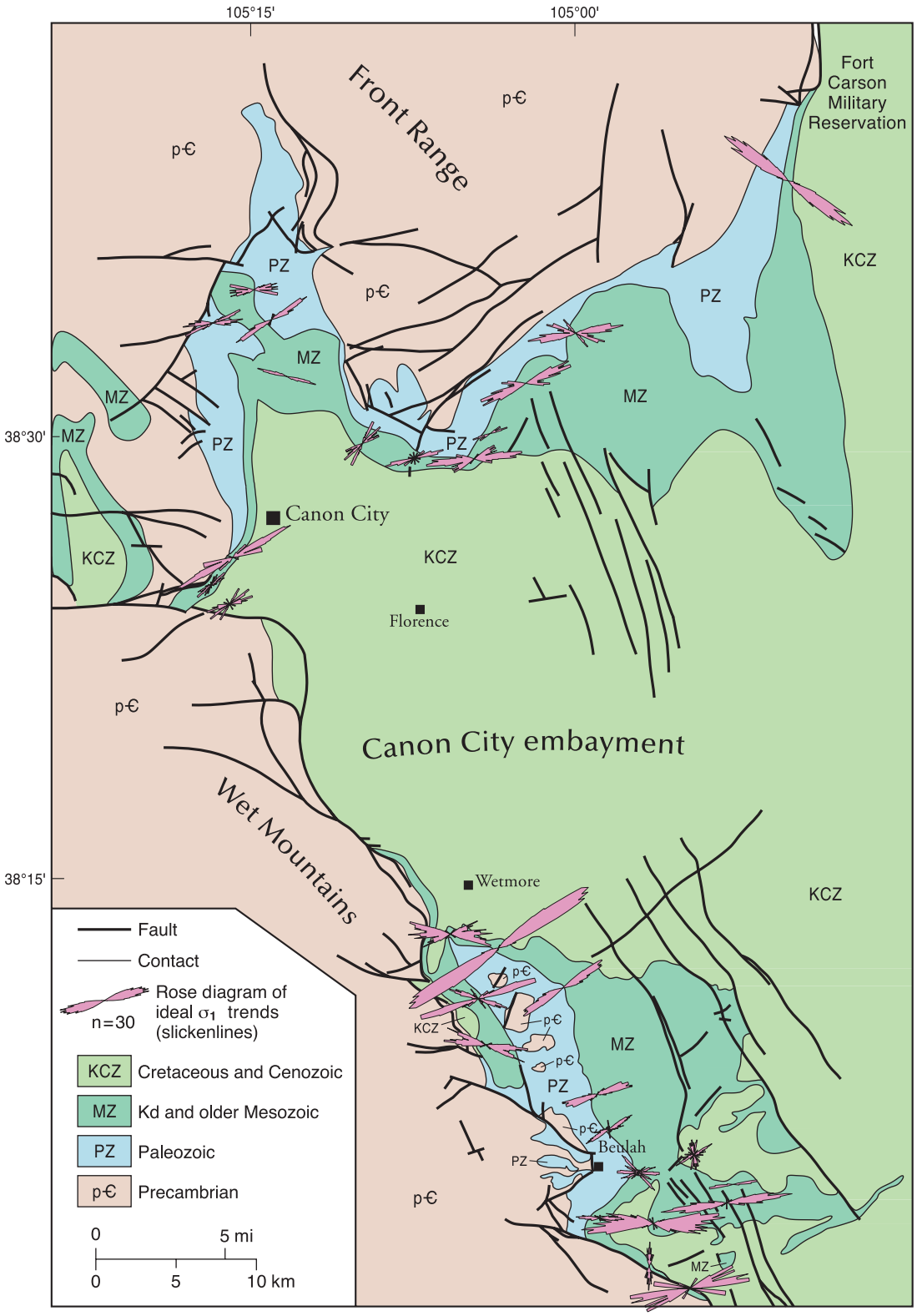

FIGURE 11—Simplified geologic map of the southern margin of the Front Range and the Canon City embayment after Tweto (1979). Smoothed rose diagrams show ideal σ_1 axis trends for individual localities with slickensided faults from Jurista (1996).

faults are considerable judging by the existence of thrust windows bowed up by post-Laramide plutons. These windows expose Pierre Shale 9 km from the Williams Range thrust front east-southeast of Dillon, Colorado (Fig. 13; Ulrich 1963), and 10 km from the Never Summer thrust front north of Granby (O'Neill 1981).

The thrust nature of the low angle faults has not been debated in recent years, although Chapin (1983) suggested that they might conceal underlying and adjacent strike-slip faults. Chapin (1983) suggested two zones of potential strike-slip deformation in the western Front Range that might transfer right-lateral slip from the Echo Park and Ilse

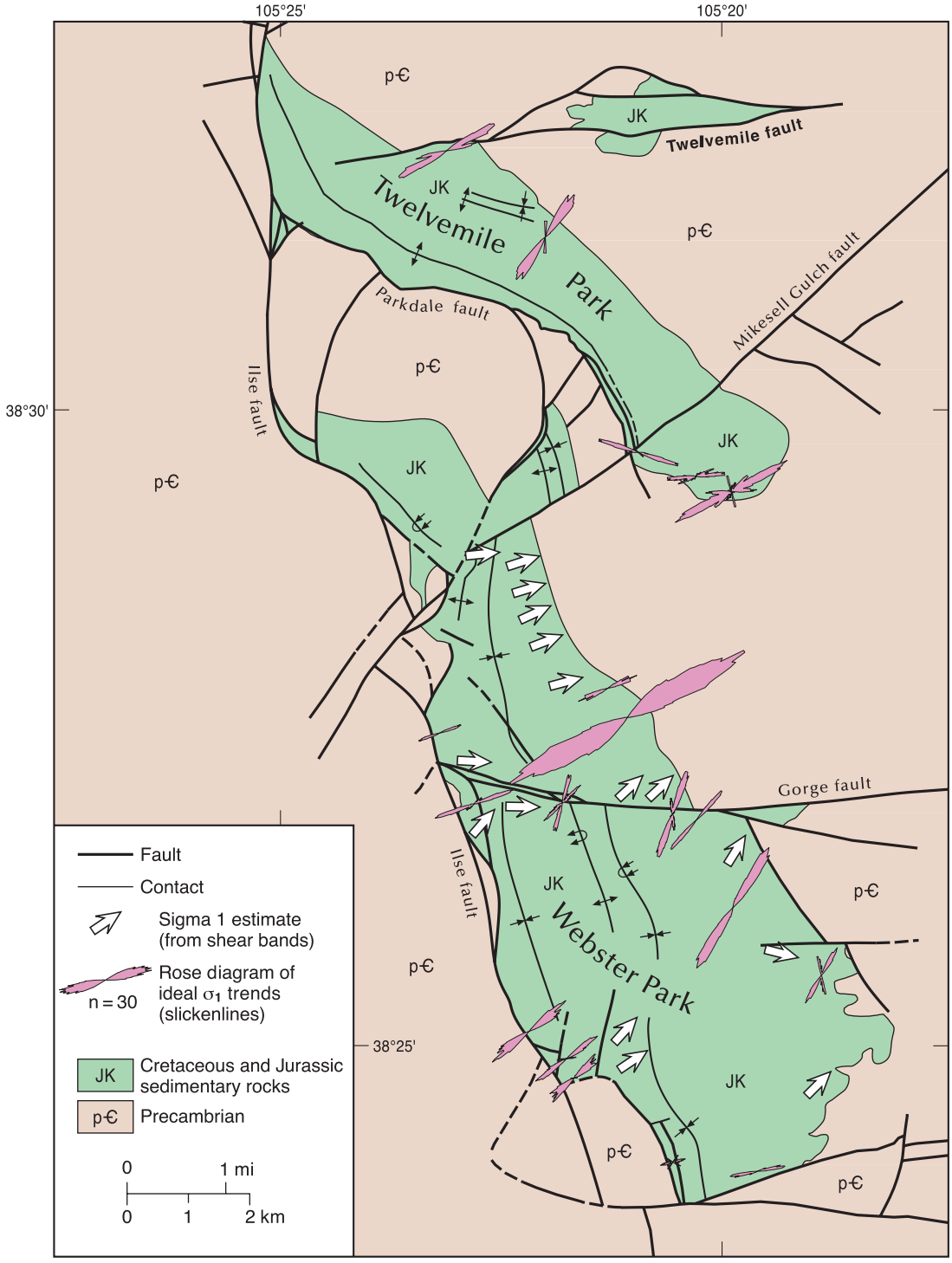

FIGURE 12—Simplified geologic map of the Webster Park–Twelvemile Park area south of the Front Range in the Wet Mountains after Tweto (1979). Smoothed rose diagrams show ideal σ_1 axis trends for individual localities with slickensided faults and arrows show average compression axes derived from shear bands (Fryer 1997).

fault systems to Wyoming. They are the Mt. Bross fault system, a north-northwest-striking zone of faults with right-lateral separations transecting the Middle–North Park Basin, and a north-striking zone of deformation north-northwest of Granby, Colorado, which continues north in the Laramie Basin of Wyoming (Figs. 1, 13).

The Mt. Bross fault west of Granby dips east, bringing Pierre Shale over Middle Park Formation (Izett 1968). It forms the western margin of the Breccia Spoon syncline, which is clearly defined by cliffs of the volcaniclastic Paleocene Windy Gap member of the Middle Park Formation. Izett (1968) interpreted the Mt. Bross fault as a reverse fault, a hypothesis that was challenged by Chapin (1983) who noted the presence of en echelon folds associated with the northern extension of the Mt. Bross fault.

The entire western slope of the Front Range is complicated by an active post-Laramide history. Mid-Tertiary volcanic rocks and plutonic bodies are abundant and appear to fol-

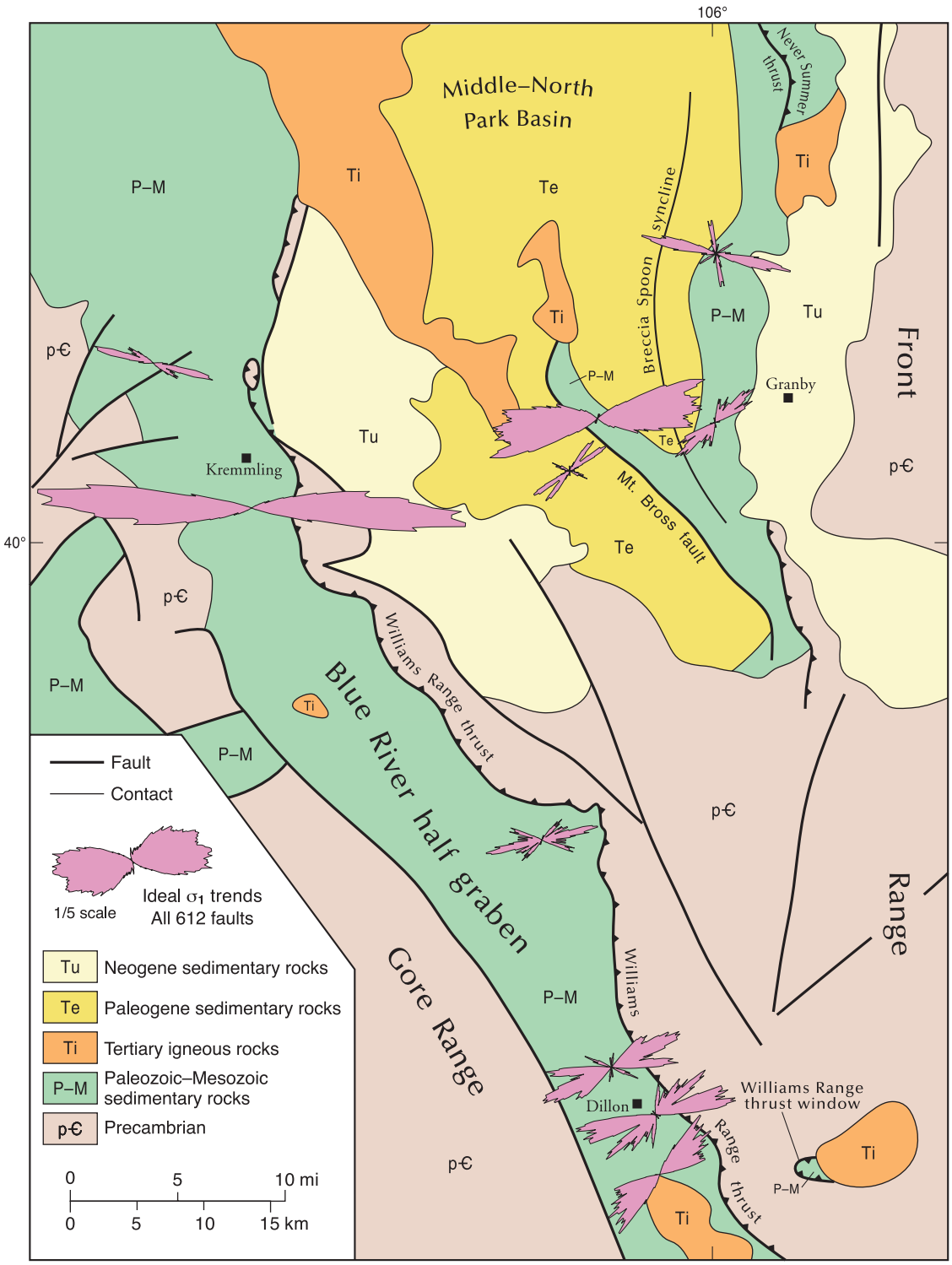

FIGURE 13—Simplified geologic map of the west-central Front Range after Tweto (1979). Smoothed rose diagrams show ideal σ_1 axis trends for lumped localities (see appendix for individual locality information).

low the margin of the Front Range northward. The aptly-named Troublesome Formation is well dated by mammal fossils and volcanic ash with fission track ages between 20 and 13 Ma (Izett and Barclay 1973). Near Kremmling (Fig. 13), it was deposited in localized extensional basins whose faults follow Laramide thrust traces. This suggests that the Troublesome Formation may have been deposited in localized basins caused by back-sliding on thrust faults (Izett and Barclay 1973). Later tilting of Pliocene basalt flows is consistent with Neogene normal faulting along the Blue River half graben, the northern extension of the Rio Grande rift (West 1978; Kellogg 1999).

Minor faults can be difficult to find in the west slope of the Front Range due to more extensive weathering and vegetative cover resulting from the increased precipitation on

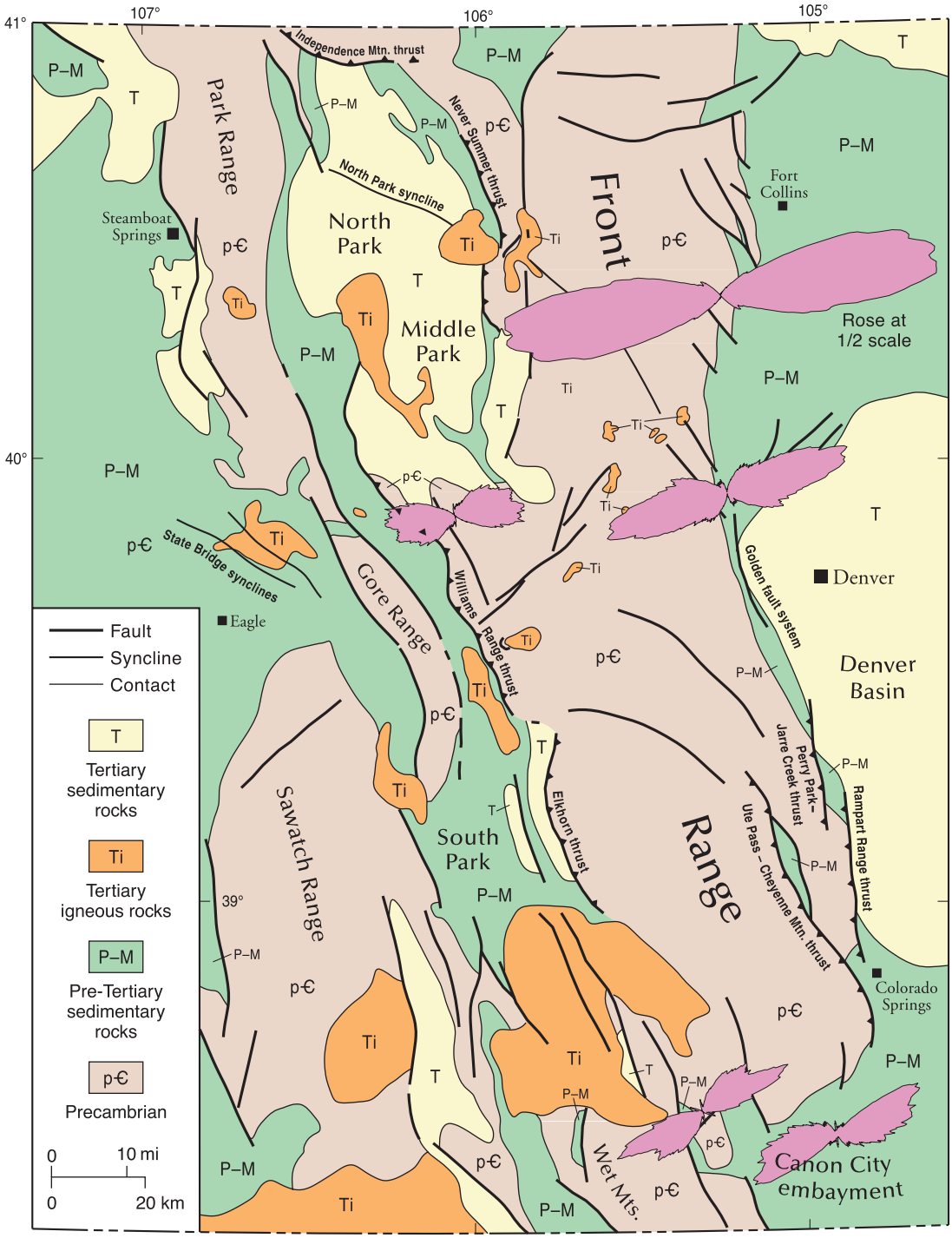

FIGURE 14—Geologic map of the Colorado Front Range (simplified from Tweto 1979) with rose diagrams of ideal σ_1 axis trends for each study area. The rose diagrams are scaled according to the number of measurements (see Table 1) except for diagram for the northeast Front Range, which is plotted at 50% scale.

the western slope. Locally, the area has extensive hydrothermal alteration associated with Laramide and post-Laramide magamtism and rifting. Areas without major river systems, such as South Park, can be particularly frustrating because of the lack of fresh exposures with slickensided surfaces. Many field days in South Park yielded only a few east-dipping thrust planes with an average slickenline trend of N75°E. Likewise, no fault planes were found in the northern part of the North Park Basin. These areas do not lack deformation, as seismic profiles from both basins show intense faulting and folding. Rather, minor faults just do not hold up well in natural outcrops under these weathering conditions. In addition, the west slope of the Front Range has less area of exposed Cretaceous sandstones, the most productive strata in terms of slickenside preservation to the east.

Another complication is provided by Neogene extension along the northern Rio Grande rift. High-angle normal faults can be easily excluded from the minor fault data but associated strike-slip faults are included in our data sets. Recent work on Neogene extension (Finnan and Erslev

2001) has identified at least two orientations of extension: 1) northeast-southwest extension with associated north-striking left-lateral and northwest-striking right-lateral faults, and 2) eash-west extension, possibly with associated north-northwest-striking right-lateral and north-northeast-striking left-lateral faults. A mysterious, north-northeast-trending shortening event, with north-striking right-lateral and northeast-striking left lateral faults (Wawrzyniec et al. 1999; Erslev et al. 1999; Erslev 2001), may be related to Neogene east-west extension. But cross-cutting relationships on north-striking faults commonly show strike-slip slickenlines overprinted by normal fault slickenline, suggesting a separate phase of post-Laramide strike-slip faulting. This possibility is supported by Neogene west-northwest-trending folds at State Bridge and North Park (Fig. 13; Erslev 2001).

There are two areas with good exposures of Cretaceous sandstones in the west slope: near Dillon, Colorado, west of Denver (Kellogg 1997) and along the Colorado River near Granby and Kremmling (Fig. 13). Maxima of fault poles, slickenlines and ideal σ_1 axes (Fig. 3e) are similar to those from the northeastern Front Range (Figs. 3a), indicating conjugate thrust and strike-slip faulting about common east-northeast-trending shortening and compression axes. Rose diagrams of west slope slickenline trends (Fig. 4e), however, show more variability for thrust and strike-slip fault types, resulting in a broad array of ideal σ_1 axis trends.

Rose diagrams of ideal σ_1 axes for three different subareas exposing Dakota sandstone near Dillon (Fig. 13) show complex, multi-mode orientations with an average east-northeast orientation. In several spots, east-northeast-trending thrust fault slickenlines are overprinted by north-northeast-trending thrust fault slickenlines. Additional complexity is added by younger normal faulting of the Blue River half graben, which may contribute some of the strike-slip slickenlines.

To the north-northwest, one third of the way from Dillon to Kremmling, exposures of sandstones with the Pierre Shale below the well-delineated Williams Range Thrust at Ute Pass (Figs. 13, 5c) show a complex array of strike-slip and thrust faults. The two localities sampled gave average ideal σ_1 axis trends of N62°E and S67°E. In combination with the faults from the Dillon area, this data suggests shortening and compression roughly normal to the Williams Range thrust. Further north, near Kremmling at outcrops on the road to Gore Pass and at exposures in Gore Canyon, strike-slip slickenlines (including two localities from Ehrlich 1999) indicate east-trending to east-southeast trending shortening and compression oblique to the general east-northeast dips of the major faults and the sedimentary strata.

Along the Colorado River between Kremmling and Granby, complex faulting shows multiple orientations of shortening and compression. The Windy Pass member of the Middle Park Formation spans the Cretaceous–Paleocene boundary and is locally composed of highly-indurated, very coarse grained volcaniclastic strata that probably originated from Laramide stratovolcanoes of the Colorado Mineral Belt (Izett 1968). Conjugate thrust and strike-slip faults at a locality on the west side of the Breccia Spoon syncline next to the Mt. Bross fault (Figs. 13, 5d) show two modes of ideal σ_1 axes, a major east-northeast mode and a minor east-southeast mode. The east-northeast mode is nearly perpendicular to the Mt. Bross fault, suggesting thrust motion. The east-southeast mode is oblique to the fault and parallels ideal σ_1 axis modes west of Kremmling.

The Windy Pass member on the east side of the Breccia Spoon syncline also contains excellent slickensides (see rose diagram closest to Granby in Fig. 13), although the 80° dip of the strata makes their interpretation more difficult. Here, individual thrust planes locally show two slickenside lineations with north-northeast-trending slickenlines overprinting northeast and east-northeast slickenlines.

A key locality north-northwest of Granby (stop B2 in Erslev et al. 1999) exposes mixed volcaniclastic and arkosic components (from Front Range crystalline rocks) in the Paleocene Middle Park Formation (Izett 1968). Three fault sets are exposed—early thrust faults with northeast- and west-northwest-trending ideal σ_1 axes and late strike-slip faults with north-northwest-trending ideal σ_1 axes. The later set of faults is probably post Laramide since they roughly parallel strike-slip, north-striking faults (Fig. 4f) which cut the 29 Ma (K-Ar; Corbett 1964) Mt. Richtofen batholith (O'Neal 1981) north of Granby at Cameron Pass. The post-Laramide age of these faults is confirmed by the fact that the batholith cuts Laramide thrusts forming the western margin of the Front Range arch.

Discussion and conclusions

Minor faults within Cretaceous and Paleocene units flanking the Front Range are strongly dominated by thrust and strike-slip faults indicating east-northeast-trending shortening and compression. The most tightly defined ideal σ_1 axes, as documented by the eigenvectors in Table 1, come from the northeastern Front Range, where en echelon map-scale faults transect the north-trending range front. Some local control of fault strains and stresses is evident in a weak correlation of ideal σ_1 axes with changes in the dip directions of the Phanerozoic strata. The least well-defined ideal σ_1 axes come from the complex transition area of the east-central Front Range northwest of Denver. In this area, the dispersion of fault data appears to be related to the steeper inclination of the strata, which suggests that early-formed faults were rotated by subsequent deformation. In addition, the northwest-southeast thrust faulting east of the range front was probably caused by gravity sliding associated with the Wattenberg high.

Ideal σ_1 axes from the southern and western flanks of the Front Range are more diffuse than those from the northeastern Front Range, with their first eigenvalues ranging between 0.64 and 0.67 as compared to 0.72 for the northeast Front Range (Table 1). The two study areas in the southern plunge of the range have asymmetrical distributions of ideal σ_1 axes with opposite senses of asymmetry. For the Canon City embayment, a clockwise asymmetry relative to the primary east-northeast mode can be ascribed to local influences. Strata at stations with more east-west slickenlines and ideal σ_1 axes typically dip to the southeast, suggesting that southeast-directed gravitational sliding and/or folding combined with east-northeast tectonic stresses to control fault orientations at these localities (Jurista 1996). In the Webster Park area, the counterclockwise asymmetry of slickenlines and calculated σ_1 axes relative to the primary east-northeast mode can be ascribed to stress refraction adjacent to map-scale strike-slip faults. Most stations with more northeasterly ideal σ_1 axes are within 1 km of these faults, and their deviations relative to the primary N60°E mode increase as the faults are approached (Fryer 1997).

The distribution of fault types is quite variable. For the northeast Front Range (Fig. 4a), approximately equal proportions of thrust, left-lateral and right-lateral faults suggests pure shear shortening. The abundance of strike-slip faults is surprising, considering the scarcity of parallel map-scale faults, and indicate a component of horizontal elongation perpendicular to average shortening orientations. An analogous situation may be the minor faulting associated with the Northridge earthquake of 1994, in which thrust faulting at depth caused strike-slip faulting and fold axis-parallel extension in the hanging wall (Hudnut et al. 1996;

Unruh and Twiss 1998). A similar fault type distribution also is present in the Canon City embayment (Fig. 4c), an area which is also underlain by a system of southwest-directed backthrusts (Jurista 1996).

In contrast, thrust and reverse faults dominate the minor faults in the east-central Front Range and Webster Park areas. Both of these areas are more immediately adjacent to major thrust systems, the Golden and Ilse fault systems, which may explain the dominance of minor thrust faults. On the western part of the range, strike-slip faults become more dominant farther from the major thrust faults.

Slickenline and ideal σ_1 axis orientations give valuable information on the type of strain during the Laramide orogeny. In the central and southern Front range, the general symmetry of major thrust faults with respect to the range suggests a pure shear pop-up structure (Fig. 2c; Raynolds 1997). In the northern Front Range, surface faults are directed mostly to the west-southwest, although wedge models (e.g., Fig. 2d) suggest that overall transport was to the east-northeast.

If simple shear occurred in the horizontal plane due to strike-slip faulting, as proposed by Chapin (1983) and Cather (1999a), a consistent and substantial obliquity between the average slickenline and ideal σ_1 axis trends might be expected. This is the case for post-Laramide strike-slip faulting in northern New Mexico (Fig. 4f; Erslev 2001) where right-lateral faults dominate late stage deformation. In the Front Range, however, the closeness of average slickenline and ideal σ_1 axis trends (Table 1) suggests that pure shear shortening dominated Laramide Front Range deformation. The only exception to this generalization is in the eastern Front Range northwest of Denver, where the difference between the N87°E-trending average slickenline and N75°E-trending average ideal σ_1 axes suggests a component of left-lateral motion. One degree differences between average slickenline and ideal σ_1 axis trends in the northeastern Front Range and Canon City embayment could be used to argue for a component of left-lateral shear. But the 2 and 3 degree differences for the Webster Park and west-central Front Range areas suggest right-lateral shear, indicating that differences between average slickenline and stress axes may be more a function of non-representative data collection than a consistent asymmetry of deformation.

These results provide a clear test of Laramide models for the development of the Colorado Front Range. The overwhelming predominance of minor faults indicating horizontal shortening and compression provides additional falsification of vertical tectonic models (e.g., Fig. 2a) invoking dip-slip on high-angle reverse and normal faults. Upthrust models using concave downward fault geometries to link surface thrusting with vertical tectonics in the lower crust (e.g., Fig. 2b) could be thought to be consistent with the fault data, but they are impossible to balance at depth. In general, horizontal shortening in the upper crust is geometrically incompatible with purely vertical slip causing a lack of horizontal shortening in the lower crust without calling for an unrealistic amount of basement expansion during uplift. One could conceive of major shallow extension to balance the shallow horizontal shortening, perhaps in the center of the arch, but there is no evidence of extension of the required magnitude (e.g., Kelley and Chapin 1997).

The possibility of regionally significant multi-stage, multi-directional Laramide slip is supported only by a few locations in the northeastern Front Range and by locations in the western Front Range. In the northeastern Front Range, west-northwest-trending slickenlines overprint east-northeast-trending slickenlines in three localities. In the western Front Range, these slip orientations are also seen, and are overprinted by both north-striking normal and strike-slip faults which cut Neogene strata. A vague bimodality in ideal σ_1 axis trends from the west-central Front Range (Fig. 4e) is permissive of multi-directional Laramide deformation, but the extensive evidence for multiple important stages of Laramide deformation seen in northern New Mexico (Fig. 5f; Chapin and Cather 1981; Erslev 2001) and southwestern Colorado (Erslev 1997; Ruf 2000) is lacking in the Front Range. Suggestions of a late northwest-southeast shortening and compression in the northern and western Front Range are supported by similar observations from northwest (Gregson and Erslev 1997) and southwest Colorado (Erslev 1997; Ruf 2000). This change in compression directions was predicted by Bird (1998) on the basis of plate trajectories but may also be due to late-stage impingement by the Cordilleran thrust belt (Gregson and Erslev 1997). The age and significance of this northwest-southeast shortening has not been well defined, although it has not been observed in post-Laramide rocks sampled to date (Finnan and Erslev 2001).

The question of whether the Front Range arch is consistent with large, north-directed, right-lateral displacements has major implications to our understanding of Laramide tectonics. The major debate over whether the geology of northern New Mexico indicates large (± 100 km: Chapin 1983; Cather 1999a) or minimal (< 20 km: Woodward et al. 1997) north-trending right-lateral separations of Laramide age is at least partially tested by fault slip in the Front Range arch. If large Laramide right-lateral displacement did occur in the Southern Rocky Mountains, there should be compatible slip on faults in central Colorado. The Front Range is a leading candidate to pass right-lateral slip from New Mexico to Wyoming because the lower amount of throw on the Gore Fault and the curvature on the Grand Hogback limits the amount of strike-slip on these structures.

Geometrically, the possibility of a component of right-lateral strike slip on concave-downward faults, forming a transpressive flower or palm-tree structure, is difficult to dismiss because of the possible movement of material in and out of the plane of section. But minor faults adjacent to faults proposed as candidates for strike-slip motion (e.g., Ilse fault, Mt. Bross fault, and faults in the northeastern Front Range) indicate shortening and compression at high angles to the fault traces. Laramide strike-slip faults are common in the margins of the Front Range, but they generally indicate shortening and compression in east-northeast-trending directions, not north-trending directions. In general, right-lateral minor faults (Fig. 4) do not parallel the north- to northwest-striking major faults that have been proposed to carry right-lateral slip northward away from New Mexico. The exceptions to this generalization occur on the western slope of the range, but these faults are more logically associated with transverse west-northwest-trending folds that deform the post-Laramide Browns Park and North Park Formations of Miocene age (Erslev et al. 1999; Wawrzyniec et al. 1999; Erslev 2001).

In addition, major northward motion of the Colorado Plateau during the Laramide would suggest much more northerly slip directions than the east-northeast–west-southwest average slip directions given in Table 1. This could be explained by strain partitioning (Cather 1999b), where separate thrust and strike-slip systems develop about separate strain axes. Cather (1999b) argued that many Laramide structures may have been influenced by pre-existing weak faults which caused strain partitioning, and this is demonstratively true along the San Andreas fault (e.g., Zoback et al. 1987). Recent work on oblique Laramide arches where there is strong geometric evidence for oblique slip (Owl Creek Arch and Casper Mountain: Molzer and Erslev 1995; Uinta arch: Gregson and Erslev 1997; San Juan Basin:

Erslev 1997; Ruf 2000; Erslev 2001), however, indicates that their slickenline trends are, on average, oblique to the arches and do not indicate strain partitioning. In each case, major sets of strike-slip or oblique-slip slickensides parallel frontal faults of the arch, confirming an oblique slip origin. This is not the case, however, for our Front Range measurements, which show that the minor faults paralleling the major range-bounding faults typically are dip-slip thrust faults.

It can be argued that thrust slip on the margins of the Front Range and Wet Mountain arches does not eliminate the possibility of major strike-slip in the interior of the arch where exposures are dominated by Precambrian crystalline rocks. A study of Precambrian contacts in the geological map of Colorado (Tweto 1979) shows only minor opportunities for significant right-lateral strike-slip separations in the internal part of these arches. For instance, the Late Precambrian Iron Dike (Chapin 1983) cuts diagonally across the Front Range arch from Denver to North Park, with the only possible separations at the western arch flank. The contacts of the Pikes Peak and Silver Plume batholiths show very little leeway for major dextral fault separations on the central and southern part of the Front Range arch. In addition, for those fault zones that do show possible separations, many of them (e.g., the Ilse Fault of the Wet Mountains) intersect the sedimentary strata at the southern plunge of the arches where hogbacks of Phanerozoic strata show no major separations. Thus it appears that there is no room for major north-directed, right-lateral strike-slip in the Front Range of Colorado.

There is, however, evidence for a minor component of oblique slip on many major faults in the Front Range area. Slight obliquities between the minor fault slip directions and the strike of the Ilse, Mt. Bross, and Williams Range thrusts, where ideal σ_1 axes are counter-clockwise rotated relative to the fault dip directions, suggest a small component of right-lateral strike slip. These suggestions of right-lateral slip are at least partially counterbalanced by opposite obliquities suggesting left-lateral motion between faults in the northeastern Front Range and the southern Canon City embayment. In the latter example, some of the discordance between the Wet Mountains fault and minor faults may be due to the likelihood that the Wet Mountains fault is a reactivated Ancestral Rocky Mountain structure of Pennsylvanian age.

In addition, the overall geometry of the Front Range arch relative to the average slip and ideal σ_1 axis trends does suggest a minor component of right-lateral motion. In the southern Front Range, the arch has a trend of N20°W, a trend whose normal is 10° oblique to the N60°E principal mode of fault slip and ideal σ_1 axis trends in the southern Front Range. To the north, however, the arch trends due north toward its bifurcation into the Medicine Bow and Laramie arches. In this area, slickenline and ideal σ_1 axis trends are more easterly, although still oblique to the arch axis. This change in the arch trend may generate a small component of right-lateral slip on the bounding faults in the northern Front Range. Residual northerly slip may be absorbed in the more east-west-striking faults bounding the Hanna Basin in southern Wyoming, as proposed by Cather (1999), and the Independence Mountain thrust fault (Blackstone 1977) bounding the northern margin of North Park. Still, we conclude that deformation of the Front Range arch was dominated by east-northeast–west-southwest shortening and compression, which caused major thrust faulting and subsidiary strike-slip faulting. A major challenge for the future will be the integration of the minor fault constraints into regional 3D restorations that quantify the absolute amounts of thrust and lateral slip in the Front Range of Colorado.

Acknowledgments

This research was supported by grants from the National Science Foundation (EAR-9614787 and EAR-9814698), E.G.&G. Rocky Flats, and from the donors of the Petroleum Research Fund, administered by the American Chemical Society. Student grants were provided by Geological Society of America, American Association of Geologists, Rocky Mountain Association of Geologists, and Chevron U.S.A. Insights from Donald Blackstone, Bruce Bryant, Steve Cather, Chuck Chapin, Shari Kelley, Karl Kellogg, Vince Matthews, Ned Sterne, and Donald Stone provided important additions to this work. Reviews by Steve Cather, Chuck Chapin, and Basil Tikoff are gratefully acknowledged. Finally, we would like to acknowledge the importance of the multiple roles that Chuck Chapin has played in Front Range research, from the catalytic effect of his questioning of classical Front Range structural dogma to his open-minded support of the sometimes contrary research of his colleagues.

References

Angelier, J., 1990, Inversion of field data in fault tectonics to obtain the regional stress, part 3, a new rapid direct inversion method by analytical means: Geophysical Journal International, v. 103, no. 2, pp. 363–379.

Berg, R. R., 1962, Mountain flank thrusting in the Rocky Mountain foreland, Wyoming and Colorado: American Association of Petroleum Geologists, Bulletin, v. 46, no. 11, pp. 2010–2032.

Bergh, S., and Snoke, A., 1992, Polyphase Laramide deformation in the Shirley Mountains, south central Wyoming foreland: Mountain Geologist, v. 29, no. 3, pp. 85–100.

Bird, P., 1988, Formation of the Rocky Mountains, a continuum computer model: Science, v. 239, no. 4847, pp. 1501–1507.

Bird, P., 1998, Kinematic history of the Laramide orogeny in latitudes 35°–49°, western United States: Tectonics, v. 17, no. 5, pp. 780–801.

Blackstone, D. L., Jr, 1977, Independence Mountain thrust fault, North Park Basin, Colorado: University of Wyoming, Contributions to Geology, v. 16, pp. 1–15.

Blackstone, D. L., 1990, Rocky Mountain foreland structure exemplified by the Owl Creek Mountains, Bridger Range, and Casper Arch, central Wyoming: Wyoming Geological Association, Guidebook 41, pp. 151–166.

Boos, C. M., and Boos, M. F., 1957, Tectonics of eastern flank and foothills of Front Range, Colorado: American Association of Petroleum Geologists, Bulletin, v. 41, no. 12, pp. 2603–2676.

Braddock, W. A., Connor, J. J., Swann, G. A., and Wolhford, D. D., 1988a, Geologic map of the Laporte quadrangle, Larimer County, Colorado: U.S. Geological Survey, Geologic Quadrangle Map GQ-1621, scale 1:24,000.

Braddock, W. A., Calvert, R. H., Gawarecki, S. J., and Nutalaya, P., 1970, Geologic map of the Masonville quadrangle Larimer County: U.S. Geological Survey, Geologic Quadrangle Map GQ-832, scale 1:24,000.

Braddock, W. A., Nutalaya, P., and Colton, R. B., 1988b, Geologic map of the Carter Lake Reservoir quadrangle, Boulder and Larimer Counties: U.S. Geological Survey, Geologic Quadrangle Map GQ-1628, scale 1:24,000.

Braddock, W. A., Calvert, R. H., Wohlford, D. D., and O'Connor, J. T., 1989, Geologic map of the Horsetooth reservoir quadrangle, Larimer County, Colorado: U.S. Geological Survey, Geologic Quadrangle Map GQ-1625, scale 1:24,000.

Brewer, J. A., Allmendinger, R. W., Brown, L. D., Oliver, J. E., and Kaufman, S., 1982, COCORP profiling across the Rocky Mountain front in southern Wyoming, Part 1, Laramide structure: Geological Society of America, Bulletin, v. 93, no. 12, pp. 1242–1252.

Brown, W. G., 1984, A reverse fault interpretation of Rattlesnake Mountain anticline, Big Horn Basin, Wyoming: The Mountain Geologist, v. 21, p. 3135.

Brown, W. G., 1988, Deformation style of Laramide uplifts in the Wyoming foreland; *in* Schmidt, C. J., and Perry, W. J., Jr. (eds.),

Interaction of the Rocky Mountain foreland and the Cordilleran thrust belt: Geological Society of America, Memoir 171, pp. 1–26.
Bryant, B., Marvin, R. F, Naeser, C. W., and Mehnert, H. H., 1981, Ages of igneous rocks in the South Park–Breckenridge region, Colorado, and their relation to the tectonic history of the Front Range uplift; Shorter contributions to isotope research in the western United States, 1980: U.S. Geological Survey, Professional Paper 1199-C, pp. 15–35.
Burbank, W. S., and Goddard, E. N., 1937, Thrusting in Huerfano Park Colorado, and related problems of orogeny in the Sangre de Cristo Mountains: Geological Society of America, Bulletin, v. 48, no. 7, pp. 931–976.
Byerlee, J., 1978, Friction of rocks: Pure and Applied Geophysics, v. 116, no. 4–5, pp. 615–626.
Cather, S. M., 1999a, Implications of Jurassic, Cretaceous, and Proterozoic piercing lines for Laramide oblique slip faulting in New Mexico and the rotation of the Colorado Plateau: Geological Society of America, Bulletin, v. 111, no. 6, pp. 849–868.
Cather, S. M., 1999b, Laramide faults in the Southern Rocky Mountains—a role for strain partitioning and low frictional strength strike-slip faults? (abs.): Geological Society of America, Abstracts with Programs, v. 31, no. 7, pp. A-186.
Chapin, C. E., 1983, An overview of Laramide wrench faulting in the Southern Rocky Mountains with emphasis on petroleum exploration; *in* Lowell, J. D., and Gries, R. R. (eds.), Rocky Mountain foreland basins and uplifts: Rocky Mountain Association of Geologists, pp. 169–179.
Chapin, C. E., and Cather, S. M., 1981, Eocene tectonics and sedimentation in the Colorado Plateau–Rocky Mountain area: Arizona Geological Digest, v. 14, pp. 175–198.
Chapin, C. E. and Cather, S. M., 1983, Eocene tectonics and sedimentation in the Colorado Plateau–Rocky Mountain area; *in* Lowell. J. D., and Gries, R. R. (eds.), Rocky Mountain foreland basins and uplifts: Rocky Mountain Association of Geologists, pp. 33–56.
Chase, R. B., Schmidt, C. J., and Genovese, R. B., 1993, Influence of Precambrian rock compositions and fabrics on the development of Rocky Mountain foreland folds; *in* Schmidt, C. J., Chase, R. B., and Erslev, E. A. (eds.), Laramide basement deformation in the Rocky Mountain foreland of the western United States: Geological Society of America, Special Paper 280, pp. 45–72.
Compton, R. R., 1966, Analyses of Pliocene–Pleistocene deformation and stresses in northern Santa Lucia Range, California: Geological Society of America, Bulletin, v. 77, no. 12, pp. 1361–1380.
Corbett, M. K., 1964, Tertiary igneous petrology of the Mt. Richthofen–Iron Mountain area, north-central Colorado: Unpublished Ph.D. thesis, University of Colorado 137 pp.
Daniel, C. G., Karlstrom, K. E., Williams, M. L., and Pedrick, J. N., 1995, The reconstruction of a middle Proterozoic orogenic belt in north-central New Mexico, U.S.A.; *in* Bauer, P. W., Kues, B. S., Dunbar, N. W., Karlstrom, K. E., and Harrison, B. (eds.), Geology of the Santa Fe region: New Mexico Geological Society, Guidebook, v. 46, pp. 193–200.
DeVoto, R. H., 1980, Pennsylvanian stratigraphy and history of Colorado; *in* Kent, H. C. and Porter, K. W. (eds.), Colorado Geology: Rocky Mountain Association of Geologists, pp. 71–102.
Department of Energy (DOE), 1993, Phase II geologic characterization data acquisition high resolution deep seismic; revised final report: U.S. Department of Energy, Rocky Flats Plant, 155 pp.
Ehrlich, T. K., 1999, Fault analysis and regional balancing of Cenozoic deformation in northwest Colorado and south-central Wyoming: Unpublished M.S. thesis, Colorado State University, 116 pp.
Epis, R. C., and Chapin, C. E., 1975, Geomorphic and tectonic implications of post-Laramide, late Eocene erosion surface in the Southern Rocky Mountains; *in* Cenozoic History of the Southern Rocky Mountains: Geological Society of America, Memoir 144, pp. 45–74.
Erslev, E. A., 1986, Basement balancing of Rocky Mountain foreland uplifts: Geology, v. 14, pp. 259–262.
Erslev, E. A., 1993, Thrusts, backthrusts and detachment of Laramide foreland arches; *in* Schmidt, C. J., Chase, R., and Erslev, E. A. (eds.), Laramide basement deformation in the Rocky Mountain foreland of the western United States: Geological Society of America, Special Paper 280, pp. 339–358.
Erslev, E., 1997, Multi-directional Laramide compression in the Durango area—Why?: Four Corners Geological Society, 1997 Guidebook, pp. 1–5.
Erslev, E. A. 2001, Multi-stage, multi-directional Tertiary shortening and compression in north-central New Mexico: Geological Society of America, Bulletin, v. 113, no. 1, pp. 63–74.
Erslev, E. A., and Gregson, J. D., 1996, Oblique Laramide convergence in the northeastern Front Range—regional implications from the analysis of minor faults; *in* Thompson, R. A., Hudson, M. R., and Pilmore, C. L. (eds.), Geologic excursions to the Rocky Mountains and beyond: Colorado Geological Survey, Special Publication, 11 pp.
Erslev, E. A., and Holdaway, S. M., 1999, Laramide faulting and tectonics of the northeastern Front Range of Colorado; *in* Lageson, D. R., Lester, A. P., and Trudgill, B. D. (eds.), Colorado and adjacent areas: Geological Society of America, Field Guide 1, pp. 41–49.
Erslev, E. A., Kellogg, K. S., Bryant, B., Ehrlich, T. K., Holdaway, S. M., and Naeser, C. W., 1999, Laramide to Holocene structural development of the northern Colorado Front Range; *in* Lageson, D. R., Lester, A. P., and Trudgill, B. D. (eds.), Colorado and adjacent areas: Geological Society of America, Field Guide 1, pp. 21–40.
Erslev, E. A., and Rogers, J. L., 1993, Basement-cover geometry of Laramide fault-propagation folds; *in* Schmidt, C. J., Chase, R., and Erslev, E. A. (eds.), Laramide basement deformation in the Rocky Mountain foreland of the western United States: Geological Society of America, Special Paper 280, pp. 339–358.
Erslev, E. A., and Selvig, B., 1997, Thrusts, backthrusts and triangle zones—Laramide deformation in the northeastern margin of the Colorado Front Range; *in* Bolyard, D. W., and Sonnenberg, S. A. (eds.), Geologic history of the Colorado Front Range: Rocky Mountain Association of Geologists, pp. 65–76.
Finnan, S., and Erslev, E. A., 2001, Post-Laramide deformation in central Colorado (abs.): Geological Society of America, Abstracts with Programs, v. 33, no. 5, p. A-7.
Fryer, S. L., 1997, Laramide faulting associated with the Ilse Fault system, northern Wet Mountains, Colorado: Unpublished M.S. thesis, Colorado State University, 120 pp.
Gregson, J., and Erslev, E. A., 1997, Heterogeneous Laramide deformation in the Uinta Mountains, Colorado and Utah; *in* Hoak, T. E., Klawitter, A. L., and Bloomquist, P. K. (eds.), Fractured Reservoirs: Characterization and Modeling: Rocky Mountain Association of Geologists, pp. 137–154.
Gries, R. R., 1983, North-south compression of the Rocky Mountain foreland structures; *in* Lowell, J. D., and Gries, R. R. (eds.), Rocky Mountain foreland basins and uplifts: Rocky Mountain Association of Geologists, pp. 9–32.
Gries, R. R., and Dyer, R. C., 1985, Seismic exploration of the Rocky Mountain region: Rocky Mountain Association of Geologists and Denver Geophysical Society, 300 pp.
Hamilton, W., 1988, Laramide crustal shortening; *in* Perry, W. J., and Schmidt, C. J. (eds.), Interaction of the Rocky Mountain foreland and the Cordilleran thrust belt: Geological Society of America, Memoir 171, pp. 27–39.
Hansen, W. R., 1986, History of faulting in the eastern Uinta Mountains, Colorado and Utah; *in* Stone, D. S., and Johnson, K. S. (eds.), New interpretations of northwest Colorado Geology: Rocky Mountain Association of Geologists, pp. 5–17.
Holdaway, S. M., 1998, Laramide deformation of the northeastern Front Range, Colorado—evidence for deep crustal wedging during horizontal compression: Unpublished M.S. thesis, Colorado State University, 146 pp.
Hudnut, K. W., Shen, Z., Murray, M., McClusky, S., King, R., Herring, Hager, T. B., Feng, Y., Fang, P., Donnellan A., and Bock, Y., 1996, Co-seismic displacements of the 1994 Northridge, California, earthquake: Seismological Society of America, Bulletin, v. 86, part b, pp. S19–S36.
Izett, G. A., 1968, Geology of the Hot Sulphur Springs quadrangle, Grand County, Colorado: U.S. Geological Survey, Professional Paper 586, 79 pp.
Izett, G. A., and Barclay, C .S. V., 1973, Geologic map of the Kremmling quadrangle, Grand County, Colorado: U.S. Geological Survey, Geologic Quadrangle Map GQ-1115, scale 1:24,000.
Jacob, A. F., 1983, Mountain front thrust, southeastern Front Range and northeastern Wet Mountains, Colorado; *in* Lowell, J. D., and Gries, R. R. (eds.), Rocky Mountain foreland basins and uplifts:

Rocky Mountain Association of Geologists, pp. 229–244.
Johnson, R. A., and Smithson, S. B., 1985, Thrust faulting in the Laramie Mountains, Wyoming, from reanalysis of COCORP data: Geology, v. 13, no. 8, pp. 534–537.
Johnston, R. C., 1953, Areal geology around Parkdale, Fremont County, Colorado: Unpublished M.S. thesis, University of Oklahoma, 101 pp.
Jurista, B. K., 1996, East-northeast Laramide compression and shortening of the Canon City embayment, south-central Colorado: Unpublished M.S. thesis, Colorado State University, Fort Collins, 147 pp.
Kellogg, K. A., 1997, Geologic map of the Dillon quadrangle, Summit and Grand Counties, Colorado U.S. Geological Survey Open-file Report 97-738, scale 1:24,000.
Kellogg, K. A., 1999, Neogene basins of the northern Rio Grande rift—partitioning and asymmetry inherited from Laramide and older uplifts: Tectonophysics, v. 305, pp. 141–152.
Kelley, S. A., and Chapin, C. E., 1997, Internal structure of the southern Front Range, Colorado, from an apatite fission-track thermochronology perspective; *in* Bolyard, D. W., and Sonnenberg, S. A. (eds.), Geologic history of the Colorado Front Range: Rocky Mountain Association of Geologists, pp. 19–30.
Kittleson, K., 1992, Decollement faulting in the northwestern portion of the Denver Basin: The Mountain Geologist, v. 29, no. 2, pp. 65–70.
Kluth, C. F., and Nelson, S. N., 1988, Age of the Dawson Arkose, Southwestern Air Force Academy, Colorado, and implcations for the uplift history of the Front Range: The Mountain Geologist, vol. 25, no. 1, pp. 29–35.
Kulik, D. M., and Schmidt, C. J., 1988, Regions of overlap and styles of interaction of Cordilleran thrust belt and Rocky Mountain foreland; *in* Schmidt, C. J., and Perry, W. J., Jr. (eds.), Interaction of the Rocky Mountain foreland and the Cordilleran thrust belt: Geological Society of America, Memoir 171, pp. 75–98.
LeMasurier, W. E., 1970, Structural study of a Laramide fold involving shallow seated basement rock, Front Range Colorado: Geological Society of America, Bulletin, v. 81, no. 2, pp. 435–450.
Leonard, E. M., and Langford, R. P., 1994, Post-Laramide deformation along the eastern margin of the Colorado Front Range—a case against significant deformation: The Mountain Geologist, v. 31, pp. 45–52.
Logan, J. M., 1966, Structure and petrology of the eastern margin of the Wet Mountains, Colorado: Unpublished Ph.D thesis, University of Oklahoma, 283 pp.
Lovering, T. S. and Goddard, E. N., 1938, Laramide igneous sequence and differentiation in the Front Range, Colorado: Geological Society of America, Bulletin, v. 49, no. 1, pp. 35–68.
Lowell, J. D., 1983, Foreland deformation; *in* Lowell, J. D, and Gries, R. R.. (eds.), Rocky Mountain foreland basins and uplifts: Rocky Mountain Association of Geologists, pp. 1–8.
Matthews, V., III, and Sherman, G. D., 1976, Origin of monoclinal folding near Livermore, Colorado: Mountain Geologist, v. 13, no. 2, pp. 61–66.
Matthews, V., III, and Work, D. F., 1978, Laramide folding associated with basement block faulting along the northeastern flank of the Front Range, Colorado; *in* Matthews, V., III (ed.), Laramide folding associated with basement block faulting: Geological Society of America, Memoir 151, pp. 101–124.
Molzer, P., and, Erslev, E. A., 1995, Oblique convergence on east-west Laramide arches, Wind River Basin, Wyoming: American Association of Petroleum Geologists, Bulletin, v. 19, pp. 1377–1394.
Oldow, J. S., Bally, A. W., Ave Lallemant, H. G., and Leeman, W. P., 1989, Phanerozoic evolution of the North American Cordillera—United States and Canada; *in* Bally, A. W., and Palmer, A. R. (eds.), The geology of North America, an overview: Geological Society of America, v. 1A, pp. 139–232.
O'Neill, J. M., 1981, Geologic map of the Mount Richthofen quadrangle and the western part of the Fall River Pass quadrangle, Grand and Jackson Counties, Colorado: U.S. Geological Survey, Miscellaneous Investigations Map I-1291, scale 1:24,000.
Petit, J. P., 1987, Criteria for the sense of movement on fault surfaces in brittle rocks: Journal of Structural Geology, v. 9, pp. 597–608.
Prucha, J. J., Graham, J. A., and Nickelson, R. P., 1965, Basement-controlled deformation in Wyoming province of Rocky Mountain foreland: American Association of Petroleum Geologists, Bulletin, v. 49, , no. 7, pp. 966–992.
Raynolds, R. G., 1997, Synorogenic and post-orogenic strata in the central Front Range, Colorado; *in* Bolyard, D. W., and Sonnenberg, S. A. (eds.), Geologic history of the Colorado Front Range: Rocky Mountain Association of Geologists, pp. 43–48.
Ruf, J. C., 2000, Origin of Laramide to Holocene fractures in the northern San Juan Basin, Colorado and New Mexico: unpublished M.S. thesis, Colorado State University, 167 pp.
Schmidt, C. J., and Perry, W. J., Jr., 1988, Interaction of the Rocky Mountain foreland and the Cordilleran thrust belt: Geological Society of America, Memoir 171, 582 pp.
Selvig, B. W., 1994, Kinematics and structural models of faulting adjacent to the Rocky Flats Plant, central Colorado: Unpublished M.S. thesis, Colorado State University, 133 pp.
Smithson, S. B., Brewer, J. A., Kaufman, S., Oliver, J. E., and Hurich, C. A., 1979, Structure of the Laramide Wind River uplift, Wyoming, from COCORP deep reflection data and from gravity data: Journal of Geophysical Research, v. 84, no. B11, pp. 5955–5972.
Spang, J. H., and Evans, J. P., 1988, Geometrical and mechanical constraints on basement-involved thrusts in the Rocky Mountain foreland province; *in* Schmidt, C. J., and Perry, W. J., Jr. (eds.), Interaction of the Rocky Mountain foreland and the Cordilleran thrust belt: Geological Society of America, Memoir 171, pp. 41–52.
Stanton, H. I., and Erslev, E. A., 2001, Rotational fault-bend folds: an alternative to kink-band models with implications for reservoir geometry and heterogeneity (abs.): American Association of Petroleum Geologists, Annual Convention Program, p. A191.
Stearns, D. W., 1971, Mechanisms of drape folding in the Wyoming province; *in* Wyoming Tectonics Symposium: Wyoming Geological Association, Guidebook 23, pp. 82–106.
Stearns, D. W., 1978, Faulting and forced folding in the Rocky Mountain foreland; *in* Matthews, V., III (ed.), Laramide folding associated with basement block faulting in the western United States: Geological Society of America, Memoir 151, p. 1–37.
Sterne, N., 1999, Laramide fault patterns between Colorado Springs and Boulder: Rocky Mountain Association of Geologists, On-The-Rocks field trip.
Stone, D. S ., 1984, The Rattlesnake Mountain, Wyoming, debate—a review and critique of models: The Mountain Geologist, v. 21, pp. 37–46.
Stone, D. S., 1985, Seismic profiles of the Pierce and Black Hollow Fields, Weld County, Colorado; *in* Gries, R. R., and Dyer, R.C. (eds.), Seismic exploration of the Rocky Mountain Region: Rocky Mountain Association of Geologists and Denver Geophysical Society, Special Publication, pp. 79–86.
Stone, D. S., 1986, Seismic and borehole evidence for important pre-Laramide faulting along the axial arch in northwest Colorado; *in* Stone, D. S, and Johnson, K. S. (eds.), New interpretations of northwest Colorado Geology: Rocky Mountain Association of Geologists, pp.19–36.
Taylor, R. B., Scott, G. R., Wobus, R. A . and Epis, R. C., 1975, Reconnaissance geologic map of the Royal Gorge quadrangle, Fremont and Custer Counties, Colorado: U.S. Geological Survey, Geologic Quadrangle Map I-869, scale 1:62,500.
Tweto, O., 1975, Laramide (Late Cretaceous–early Tertiary) orogeny in the Southern Rocky Mountains; *in* Curtis, B. F. (ed.), Cenozoic history of the Southern Rocky Mountains: Geological Society of America, Memoir 144, pp. 1–44.
Tweto, O., 1979, Geologic map of Colorado: U.S. Geological Survey, scale 1:500,000.
Tweto, O., 1980, Tectonic history of Colorado; *in* Kent, H. C.,and Porter, K. W. (eds.), Colorado Geology: Rocky Mountain Association of Geologists, pp. 5–10.
Tweto, O., and Lovering, T. S., 1977, Geology of the Minturn 15-minute quadrangle, Eagle and Summit counties; U.S. Geological Survey, Professional Paper 959, 96 pp.
Ulrich, G. E., 1963, Petrology and structure of the Porcupine Mountain area, Summit County, Colorado: Unpublished Ph.D thesis, University of Colorado, 205 pp.
Unruh, J. R., and Twiss R. J., 1998, Coseismic growth of basement-involved anticlines—the Northridge–Laramide connection: Geology, v. 26, pp. 335–338.
Vollmer, F., 1992, ORIENT 1.6: Shareware stereonet computer program, http://ccl.osc.edu/cca/software/UNIX/babel1-1.6/orient.shtml, accessed January 21, 2004.

Warner, L. A., 1956, Tectonics of the Colorado Front Range: American Association of Petroleum Geologists, Rocky Mountain Section, Geological Record, pp. 129–144.

Wawrzyniec, T. F., Geissman, J. G., Melker, M., and Hubbard, M., 1999, Dextral shear east of the Colorado Plateau—a kinematic link between the Laramide orogeny and Rio Grande rifting, and a new model for rift tectonics (abs.): Geological Society of America, Abstracts with Programs, v. 31, no. 7, p. A115.

Weimer, R. J., and Ray, R. R., 1997, Laramide mountain flank deformation and the Golden fault zone; *in* Bolyard, D. W., and Sonnenberg, S. A. (eds.), Geologic history of the Colorado Front Range: Rocky Mountain Association of Geologists, pp. 49–64.

West, M. W., 1978, Quaternary geology and reported surface faulting along the east flank of the Gore Range, Summit County, Colorado: Colorado School of Mines, Quarterly, v. 73, no. 2, 66 pp.

Wobus, R. A., Epis, R. C. and Scott, G. R., 1979, Geologic map of the Cover Mountain quadrangle, Fremont, Park and Teller Counties, Colorado: U.S. Geological Survey, Miscallaneous Investigations Map I-1179, scale 1:62,500.

Woodward, L. A., Anderson, O. J., and Lucas, S. G., 1997, Mesozoic stratigraphic constraints on Laramide right slip on the east side of the Colorado Plateau: Geology, v. 25, no. 9, pp. 843–846.

Ziegler, V., 1917, Foothills structure in northern Colorado: Journal of Geology, v. 25, pp. 715–740.

Zoback, M. D., Zoback, M. L., Mount, V. S., Suppe, J., Eaton, J. P., Healy, J. H., Oppenheimer, D. H., Reasenberg, P. A., Jones, L. M., Raleigh, C. B., Wong, I. G., Scotti, O., and Wentworth, C. M., 1987, New evidence on the state of stress of the San Andreas Fault System: Science, v. 238, pp. 1105–1111.